Supplementary Information

for

Lewis Pairs for Ring-Opening Alternating Copolymerization of Cyclic Anhydrides and Epoxides

He-Yuan Ji,[†] Bin Wang, *,[†] Li Pan,[†] Yue-Sheng Li*,[†,‡]

[†]Tianjin Key Lab of Composite & Functional Materials, School of Materials Science and Engineering, Tianjin University, Tianjin 300350, China

[‡]Collaborative Innovation Center of Chemical Science and Engineering (Tianjin), Tianjin 300072, China

*E-mail: binwang@tju.edu.cn (B. W.).

*E-mail: ysli@tju.edu.cn (Y. S. L.).

Table of Contents

Experimental Section

Reagents. Unless otherwise stated, all chemicals are used without further purification. Phthalic anhydride (PA), cyclohexanedicarboxylic anhydride (CHA), maleric anhydride (MA), styrene oxide (SO), $B(C_6F_5)_3$, *S*-SO and $ZnEt_2$ were purchased from Acros. Norbornene anhydride (NA), succinic anhydride (SA), propylene oxide (PO), 1,8-diazabicyclo [5.4.0]undec-7-ene (DBU), 4-dimethylaminopyridine (DMAP), extra pure xylene and decahydronaphthalene (DHN) were purchased from Energy Chemical Co. Epichlorohydrin (ECH), $Zn(C_6H_5)_2$ and extra pure 1,2-dichlorobenzene (oDCB) were purchased from Alfa Aesar. Cyclohexene oxide (CHO) and 7-methyl-1,5,7-triazabicyclo[4.4.0] dec-5-ene (MTBD) were purchased from J&K Scientific Ltd. *S*-PO was purchased from Innochem. $Zn(C_6F_5)_2$ was purchased from Sigma-Aldrich. PA was recrystallized from dry chloroform prior to use. NA, MA and SA were purified by the way of sublimation. CHO, PO, ECH, SO, *S*-PO and *S*-SO were dried over CaH_2 for 48 h, distilled, and stored under nitrogen atmosphere. DMAP was recrystallized from anhydrous ethyl acetate before use. CHA, DBU and DHN was purified over CaH_2 and then distilled in vacuum. MTBD, $CDCl_3$ and $C_2D_2Cl_4$ were dried over molecular sieves 4 Å. All manipulations were performed using a standard Schlenk technique or in a nitrogen-filled Etelux Lab2000 glovebox unless otherwise mentioned.

General bulk copolymerization procedure. In an Etelux glovebox, the appropriate amount of Lewis acid (0.036 mmol, 1 equiv.),[1] Lewis base (0.036 or 0.072 mmol) and cyclic anhydride (3.6 mmol, 100 equiv.) were added in an oven-dried tube equipped with a magnetic stir, followed by epoxide (500 equiv.). The tube was removed from the glovebox and placed in an aluminum heating block with predetermined temperature. After the defined time, crude aliquot was withdrawn from the system by pipette and monitored by ^{1}H NMR spectroscopy in $CDCl_3$ to determine monomer conversion. The reaction mixture was diluted with approximately 10 mL dichloromethanea. And then the mixture was precipitated into 100 mL of methanol acidified by hydrochloric acid with vigorous stirring, after which the methanol was filtrated. The resulting polymers were oven-dried under vacuum at 40 °C. All analyses were performed on crude samples.

General solution copolymerization procedure. In an Etelux glovebox, the appropriate amount of Lewis acid (0.036 mmol, 1 equiv.), Lewis base (0.036 or 0.072 mmol) and anhydride (3.6 mmol, 100 equiv.) were added in an oven-dried tube equipped with a magnetic stir, followed by epoxide (100 equiv.), and then, a certain amount of solvent (xylene or oDCB or DHN) were added to ensure that original anhydride concentration was consistent with the one in bulk with an 100:500 molar ratio of anhydride/epoxide. The

tube was removed from the glovebox and placed in an aluminum heating block with predetermined temperature. After the defined time, crude aliquot was withdrawn from the system by pipette and monitored by ^{1}H NMR spectroscopy in $CDCl_3$ to determine monomer conversion. The reaction mixture was diluted with approximately 10 mL dichloromethanea. And then the mixture was precipitated into 100 mL of methanol acidified by hydrochloric acid with vigorous stirring, after which the methanol was filtrated. The resulting copolymers were dried under vacuum at 40 °C. All analyses were performed on crude samples.

Determination of regioselective ring-opening of terminal epoxides. A round-bottomed flask was charged with polyesters (100 mg), THF (10 mL), MeOH (2 mL) and NaOH (4 mol/L, 2 mL). The resultant mixture was stirred at room temperature for 24 h. Then, it was concentrated to 8 mL by evaporation. The solution was extracted with ethyl acetate (10 mL × 3). The combined organic layers were dried over anhydrous $MgSO_4$; and then the mixture was filtered and evaporated to colorless or yellow oil with a spot of ethyl acetate.[2] The enantiomeric excess (*ee*) of the resultant diols was determined by gas chromatography (GC) analysis with a chiral GC column (Agilent CycloSil-B 30 m × 0.25 mm ID × 0.25 μm film). Because poly(PA-*alt*-ECH) would generate glycidol in the environment of NaOH during hydrolysis of the resultant polyesters,[3] the GC analysis did not involve poly(PA-*alt*-ECH). Retention time of diols and separation methods were showed as follows:

1,2-Propanediol: Injection temperature 275 ºC; detection temperature 275 ºC; Oven temperature 60 ºC. Retention time of *S*-1,2-propanediol = 29.1 min; Retention time of *R*-1,2-propanediol = 30.2 min.

Styrene glycol: Injection temperature 275 ºC; detection temperature 275 ºC; Oven temperature 140 ºC. Retention time of *S*-styrene glycol = 29.6 min; Retention time of *R*-styrene glycol = 31.1 min.

Methods. ^{1}H and ^{13}C NMR spectra were recorded on a Bruker Avance III 400 MHz spectrometer at room temperature in chloroform-d_1 or DMSO-d_6, and chemical shifts were referenced to an internal standard (TMS). Variable Temperature (VT) ^{1}H NMR Spectra were recorded in $C_2D_2Cl_4$ on a Bruker Advance III 400 MHz instrument. The typical procedure for an NMR tube experiment is as follows: A NMR tube was charged with $Zn(C_6F_5)_2$ (1 equiv.), DMAP (2 equiv.), PA (2 equiv.), CHO (5 equiv.) and $C_2D_2Cl_4$ (0.5 mL) in a glovebox. And then *in situ* ^{1}H NMR experiments were carried out at variable temperatures at 25, 50, 70, 90 and 110 °C, respectively. Gel permeation chromatography (GPC) analyses were carried out on a Waters 1515/2414 instrument coupled with a Waters refractive index (RI) detector with respect to polystyrene (PS) standards. The columns included a PLgel guard 50 × 7.5 mm column and three PLgel

mixed-C 300 × 7.5 mm columns. The eluent is THF with a flow rate of 1.0 mL/min at 40 °C. Samples being tested were filtered through a 0.22 μm PTFE filter. Matrix-assisted laser desorption/ionization time of flight mass spectrometry (MALDI TOF MS) study was performed at an Autoflex III smart beam mass spectrometry from Bruker company. The polymer samples were obtained by percipitating in hexane and drying under vacuum at low PA conversion without quenching. Then the crude products were dissolved in THF at an 1 mg·mL^{-1} concentration. The cationization agent was potassium trifluoroacetate compounded as 5 mg·mL^{-1} solution. And the matrix was *trans*-2-[3-(4-tert-butylphenyl)-2-methyl-2-propenylidene]malononitrile (DCTB) and was dissolved in THF at a concentration of 40 mg·mL^{-1}. Tested solution was mixed in a volume ratio of 4:1:4 of matrix, salt and polymer sample.[4] The glass transition temperatures (T_g) of polymer samples were determined at a scanning speed of 10 °C/min (from 0 °C to 180 °C) on a TA instruments DSC Q2000 with three heating cycles.

Results and Discussion

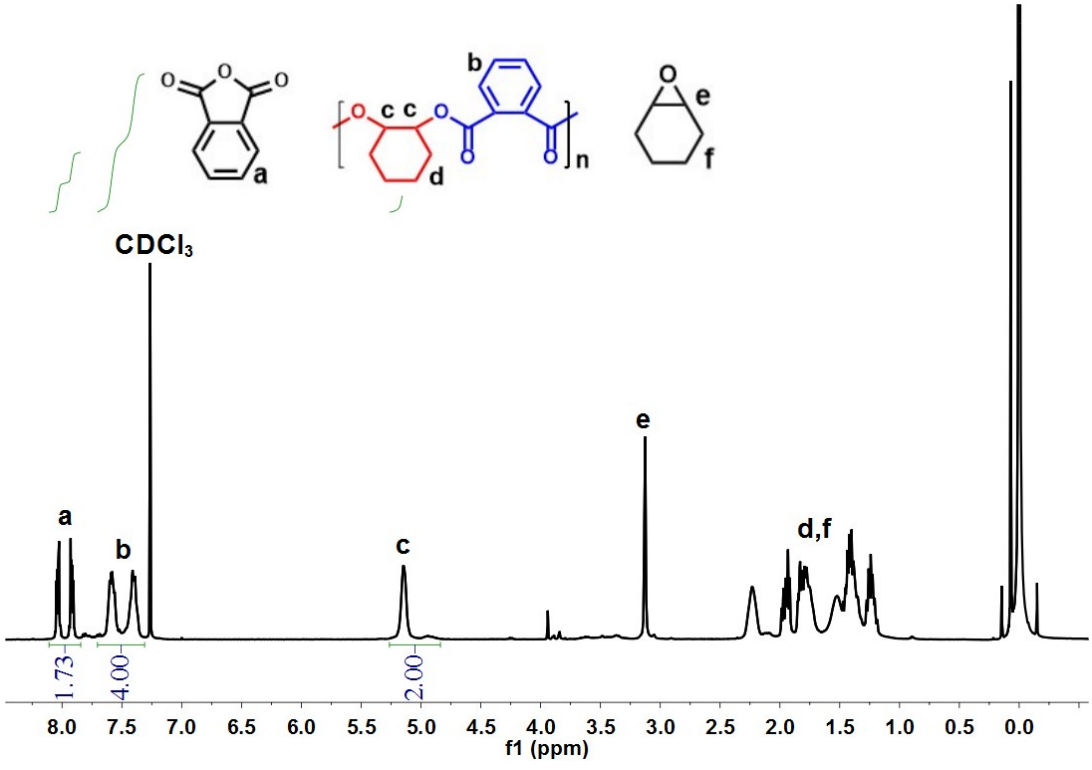

Figure S1. ^{1}H NMR spectrum of the representative crude reaction mixture of poly(PA-*alt*-CHO).

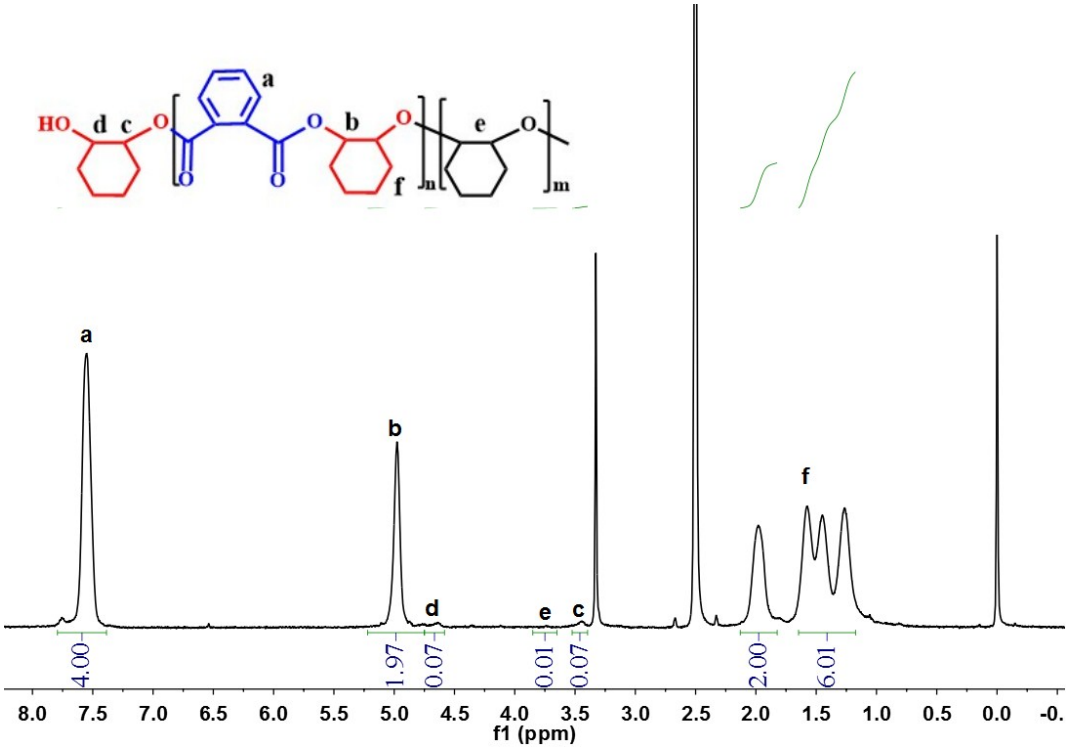

Figure S2. ^{1}H NMR spectrum of the resultant poly(PA-*alt*-CHO) by $Zn(C_6F_5)_2$/DMAP Lewis pair in DMSO-d_6. It is worth noting that the ^{1}H NMR spectra of poly(CHO-*alt*-PA) should be recorded in DMSO-d_6 rather than in $CDCl_3$, because the end group signals of resulting polyester (3.6-3.4 ppm) would overlap with the ether linkage signals (3.5-3.3 ppm) when the sample was dissolved in $CDCl_3$.[5]

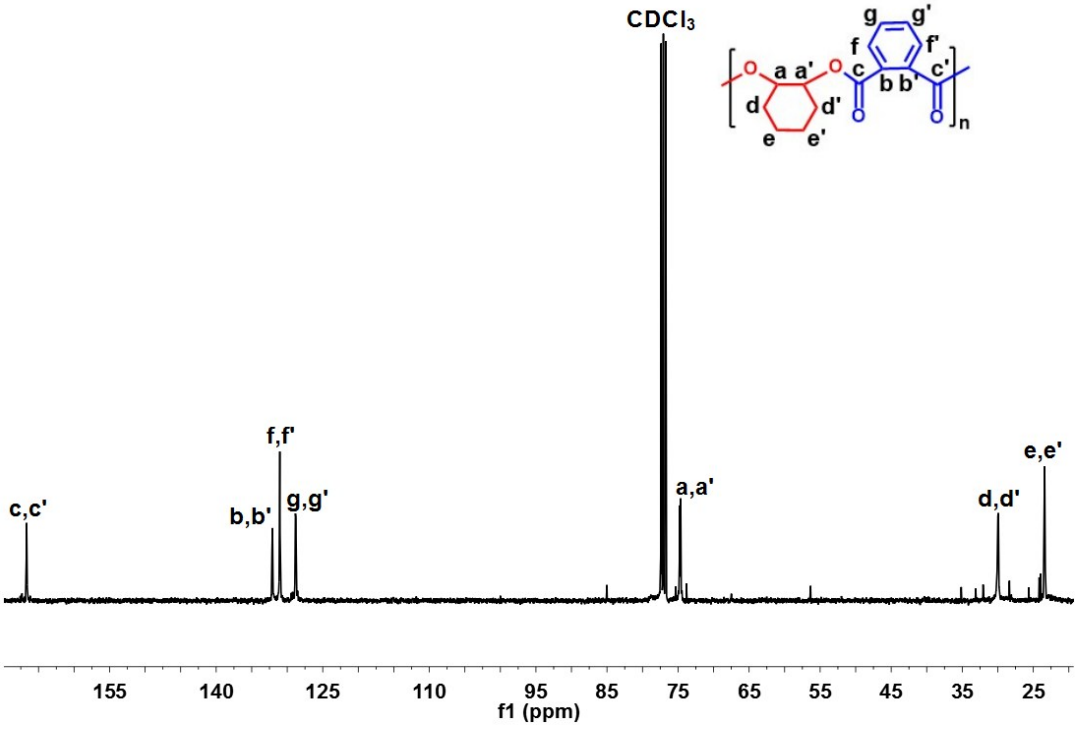

Figure S3. ^{13}C NMR spectrum of the resultant poly(PA-*alt*-CHO) in $CDCl_3$.

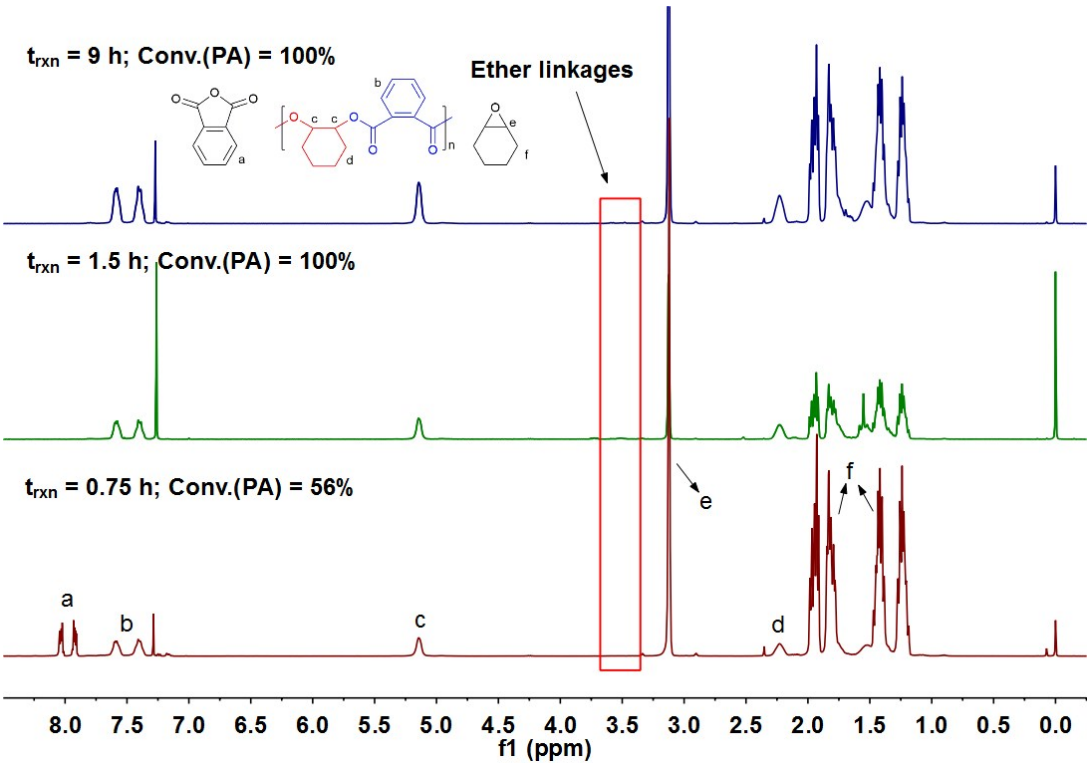

Figure S4. ^{1}H NMR spectra of the crude reaction mixture with different reaction time.

Table S1. The ROAC of PA and CHO catalyzed by frustrated Lewis pairs (FLPs).[a]

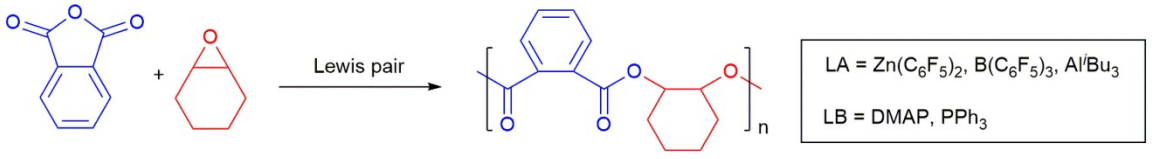

Run	Lewis pair	Temp. (ºC)	t (h)	Conv. (%)[b]	Alternating degree (%) [c]	M_n (kDa)[d]	PDI [d]
1	$Zn(C_6F_5)_2$/PPh_3	110	1	54	29	10.2	1.39
2	$B(C_6F_5)_3$/DMAP	110	0.5	57	20	15.5	1.72
3	$B(C_6F_5)_3$/ PPh_3	25	0.5	47	11	16.7	1.81
4	Al^iBu_3/DMAP	110	1	99	47	12.9	1.45

[a] Unless otherwise mentioned, the copolymerizations were carried out in neat epoxide. [b] PA conversion was determined by ^{1}H NMR. [c]Ether linkage was determined *via* ^{1}H NMR by integrating ester and ether signals). [d]M_n and PDI were determined by GPC analysis.

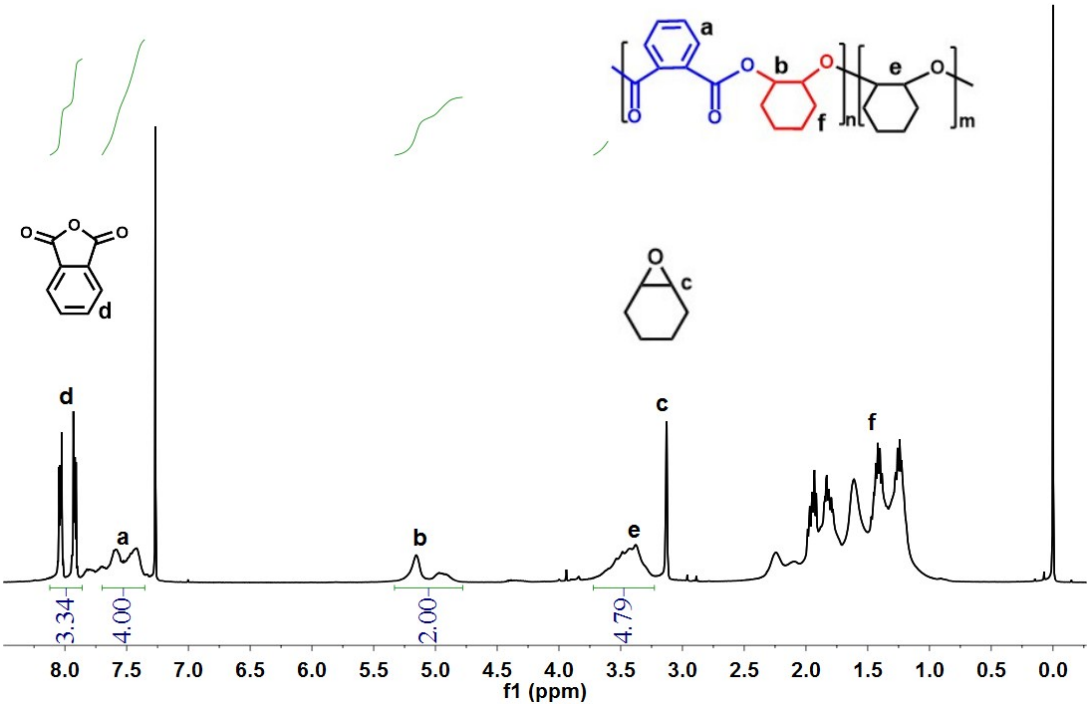

Figure S5. ^{1}H NMR spectrum of the crude reaction mixture of PA and CHO catalyzed by $Zn(C_6F_5)_2/PPh_3$ FLP in an 1:1 molar ratio in $CDCl_3$.

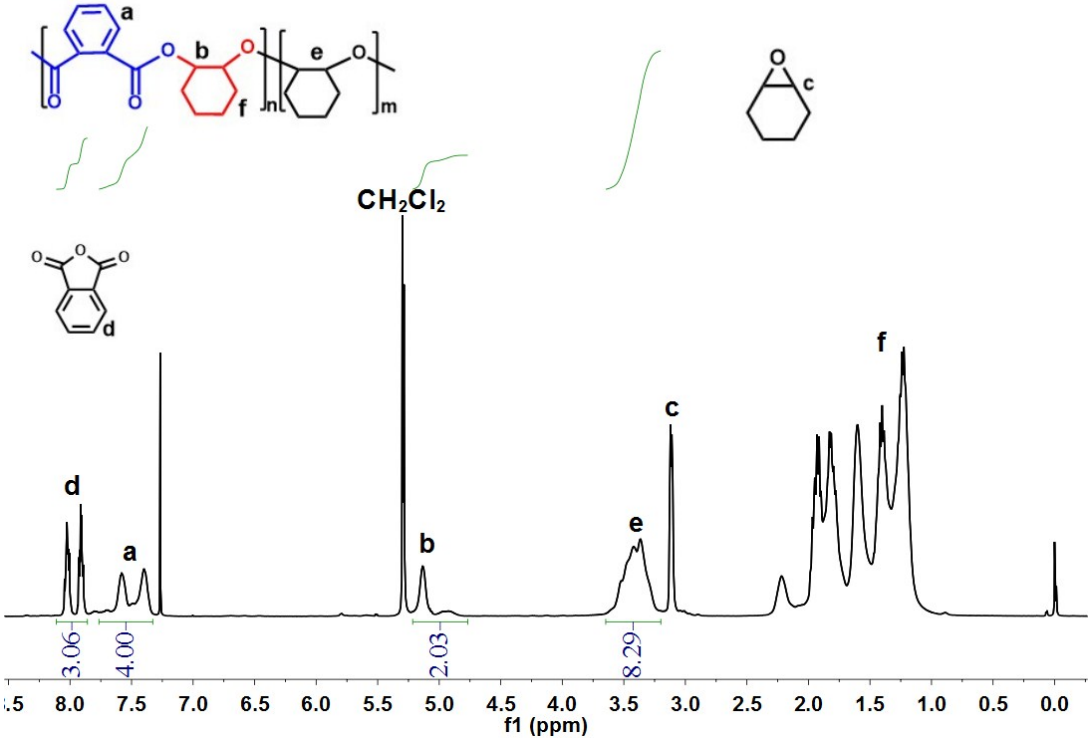

Figure S6. ^{1}H NMR spectrum of the crude reaction mixture of PA and CHO catalyzed by $B(C_6F_5)_3$/DMAP FLP in an 1:1 molar ratio in $CDCl_3$.

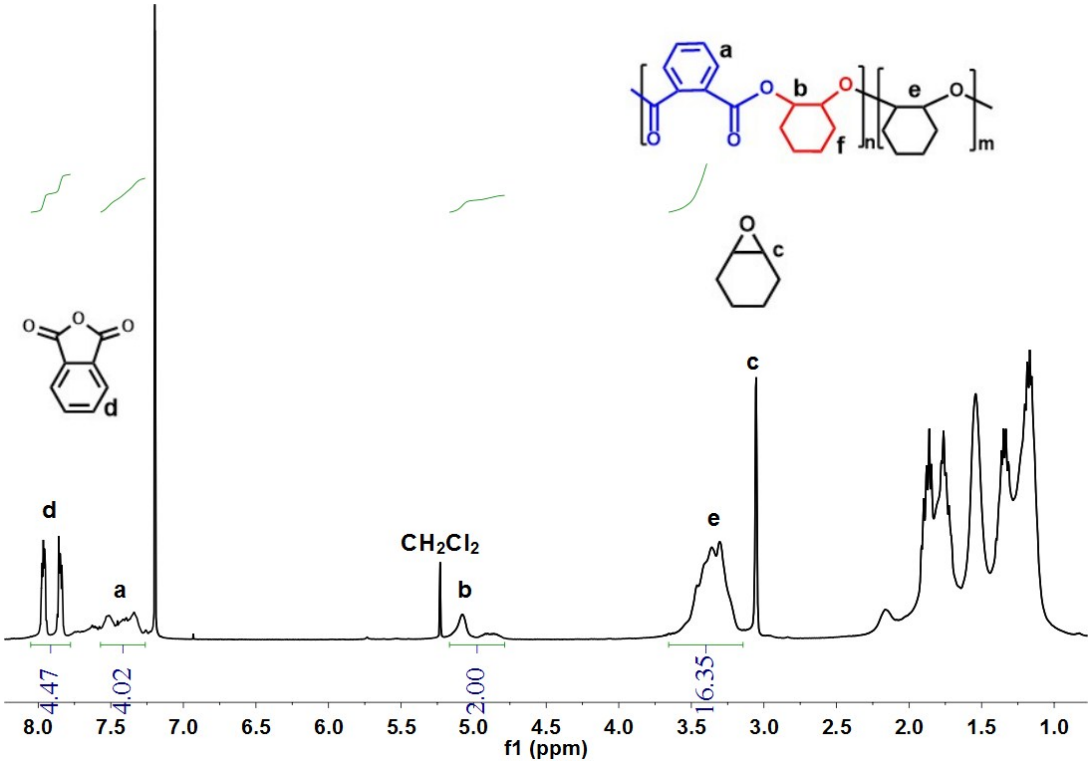

Figure S7. ^{1}H NMR spectrum of the crude reaction mixture of PA and CHO catalyzed by $B(C_6F_5)_3/PPh_3$ FLP in an 1:1 molar ratio in $CDCl_3$.

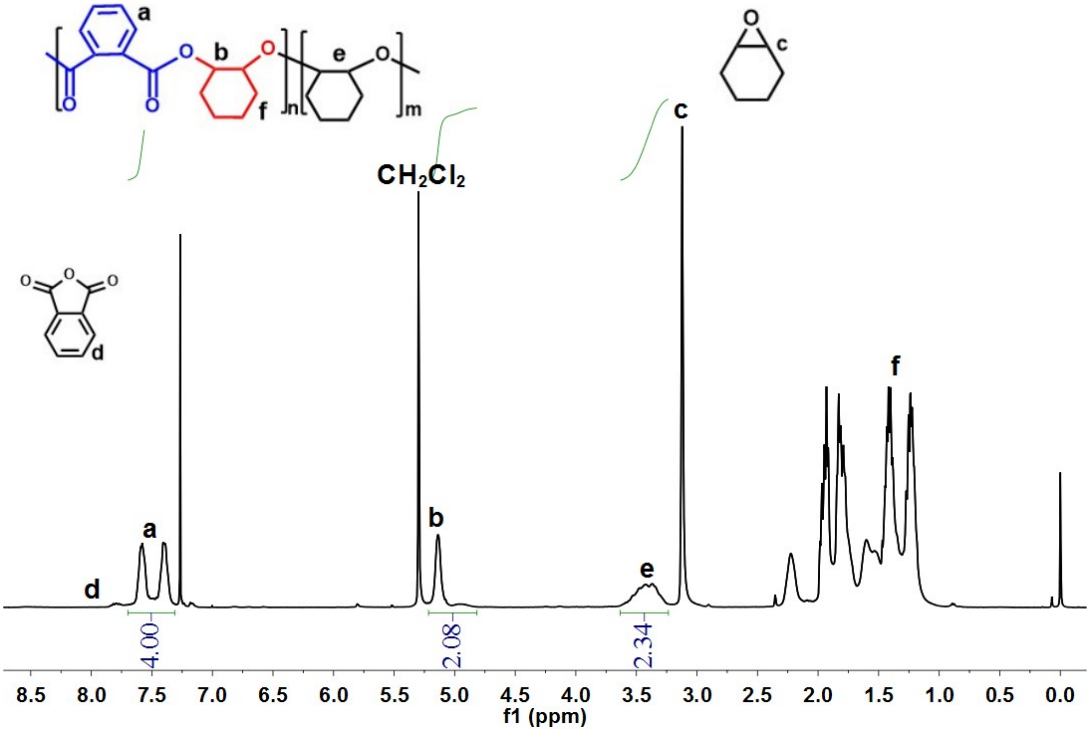

Figure S8. ^{1}H NMR spectrum of the crude reaction mixture of PA and CHO catalyzed by $Al^{i}Bu_3$/DMAP pair in an 1:1 molar ratio in $CDCl_3$.

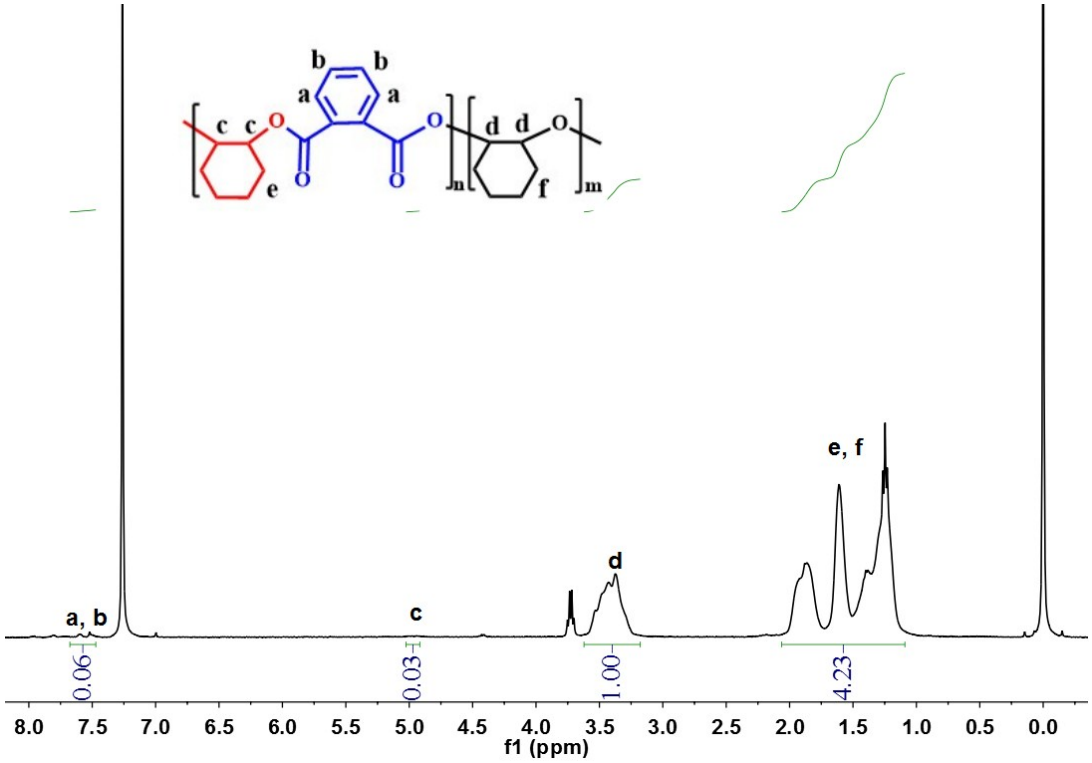

Figure S9. ^{1}H NMR spectrum of the resultant poly(PA-*co*-CHO) catalyzed by sole Lewis acid in $CDCl_3$.

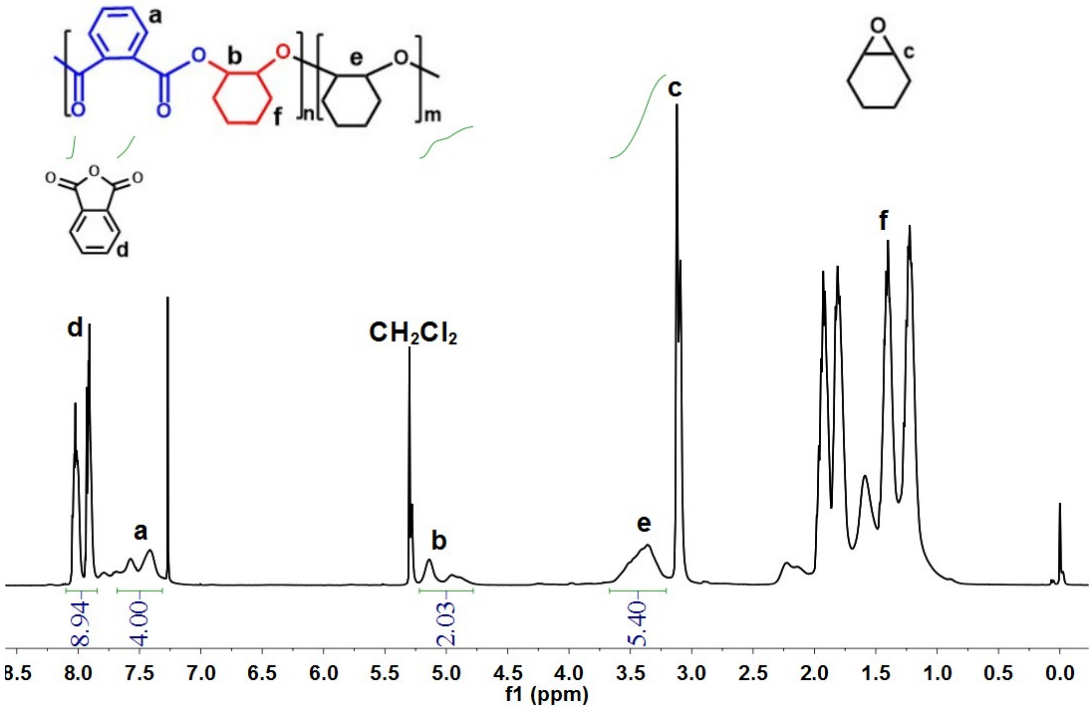

Figure S10. ^{1}H NMR spectrum of the crude reaction mixture of PA and CHO catalyzed by $Zn(C_6F_5)_2$/DMAP pair in a 2:1 molar ratio in $CDCl_3$.

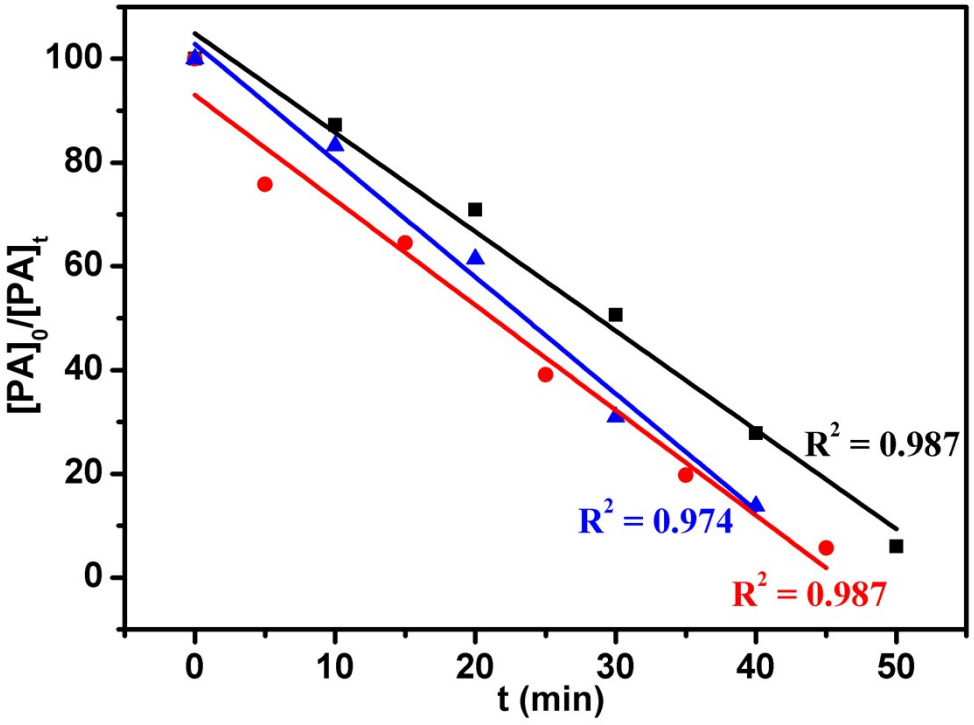

Figure S11. Zero-order kinetic plots of PA concentration for ROAC of PA and CHO in bulk at 110 ºC by using $Zn(C_6F_5)_2$/DMAP (■), $ZnEt_2$/DMAP (●), $Zn(C_6H_5)_2$/DMAP (▲) Lewis pairs in an 1:2 molar ratio.

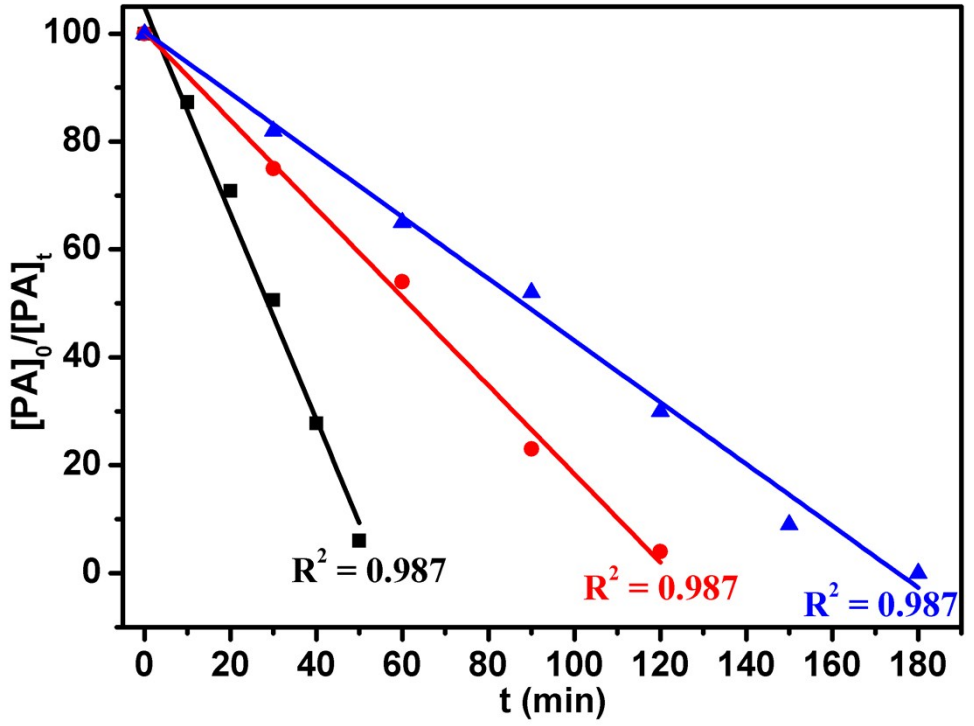

Figure S12. Zero-order kinetic plots of PA concentration for ROAC of PA and CHO in bulk at 110 ºC by using $Zn(C_6F_5)_2$/DMAP (■), $Zn(C_6F_5)_2$/DBU (●), $Zn(C_6F_5)_2$/MTBD (▲) Lewis pairs.

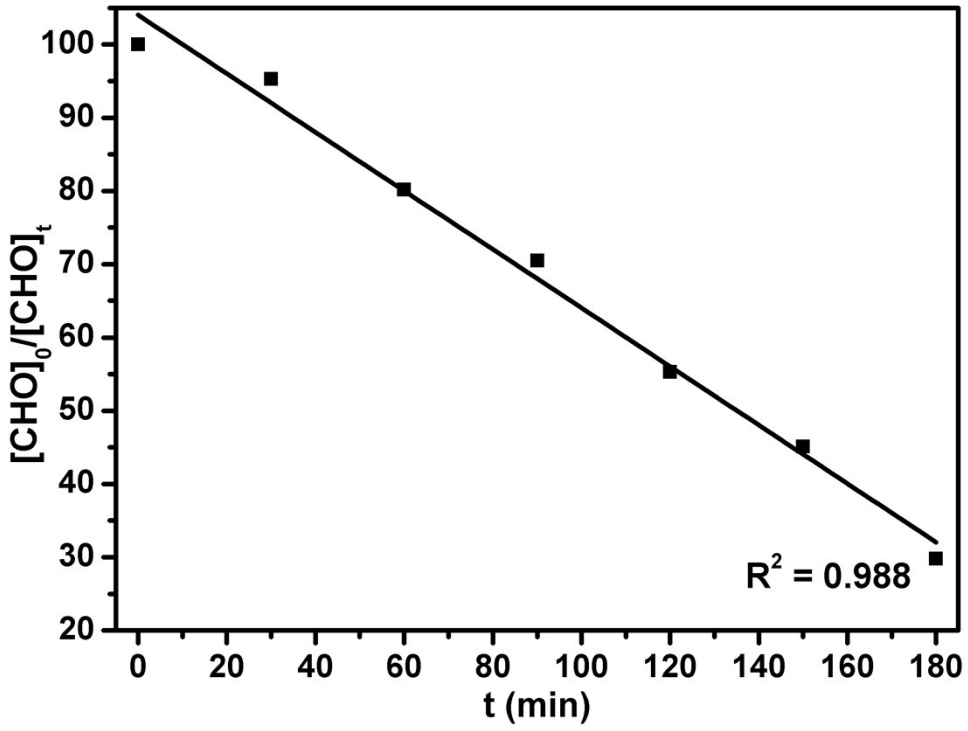

Figure S13. Zero-order kinetic plots of CHO concentration for ROAC of PA and CHO in xylene solvent at 110 ºC by using $Zn(C_6F_5)_2$/DMAP Lewis pair with molar ratio of 1:2:100:100. Original PA concentration was consistent with the one in bulk with an 100:500 molar ratio of PA/CHO. Kinetic experiment versus CHO concentration showed a lower apparent rate constant, implying that epoxide had a greater effect than anhydride on polymerization rate; and ring-opening of epoxide determined the copolymerization level (The conclusion was also proved by MALDI TOF MS in Figure 5 and S46).

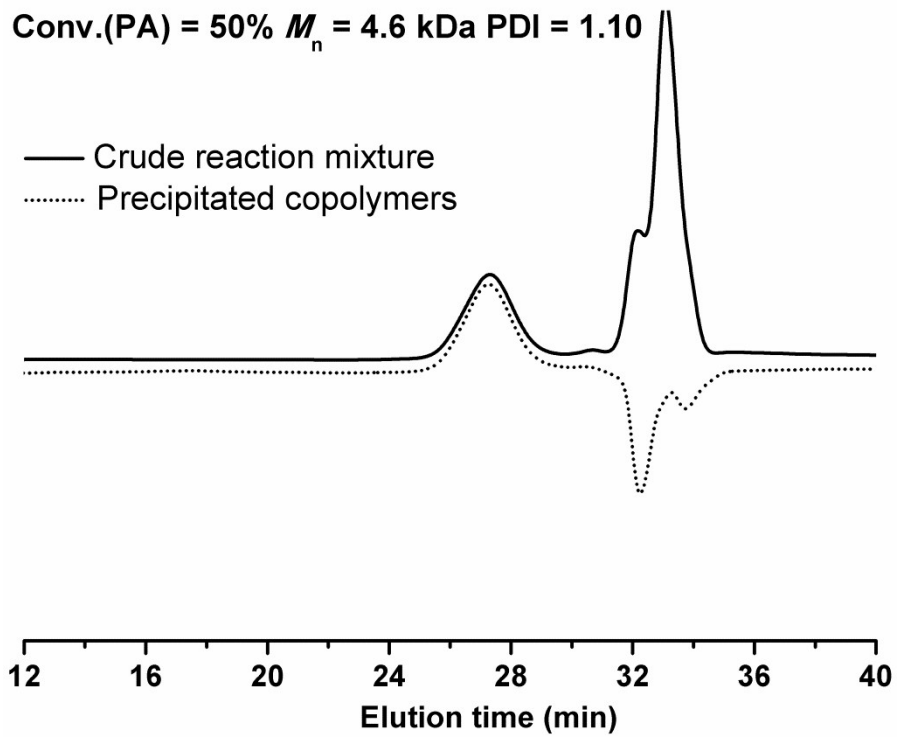

Figure S14. The GPC evolution plots of the resultant poly(PA-*alt*-CHO) obtained from crude reaction mixture (solid line) and precipitated copolymer (dot line). The unimodal GPC traces resulted from the reaction mixture of 50% PA conversion.

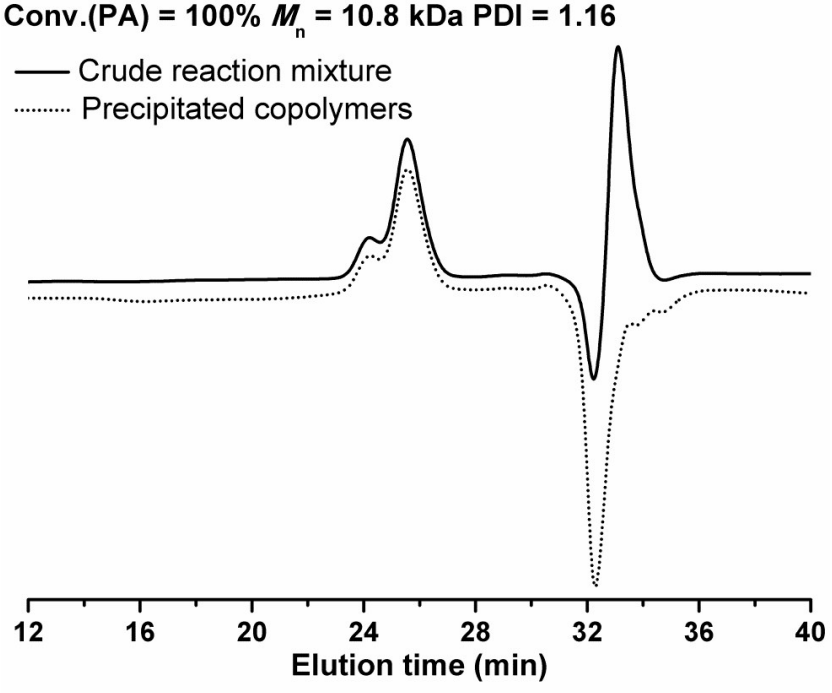

Figure S15. The GPC evolution plots of the resultant poly(PA-*alt*-CHO) obtained from crude reaction mixture (solid line) and precipitated copolymer (dot line). The bimodal GPC traces resulted from the reaction

mixture of 100% PA conversion (t_{rxn} = 2 h).

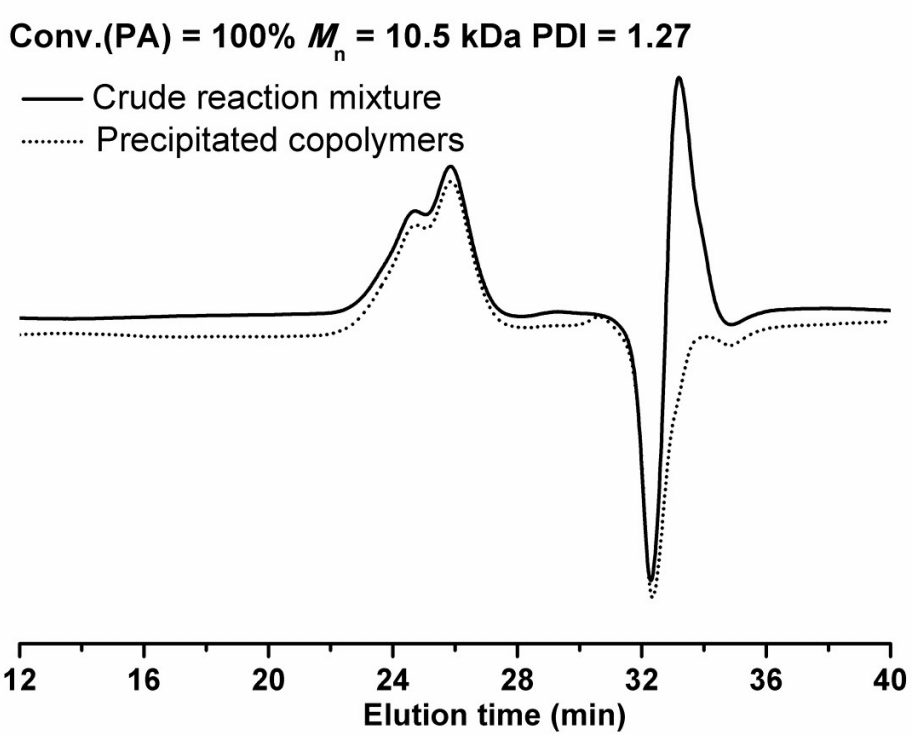

Figure S16. The GPC evolution plots of the resultant poly(PA-*alt*-CHO) obtained from crude reaction mixture (solid line) and precipitated copolymer (dot line). The wider GPC distribution appeared when reaction time was extended to 9 h.

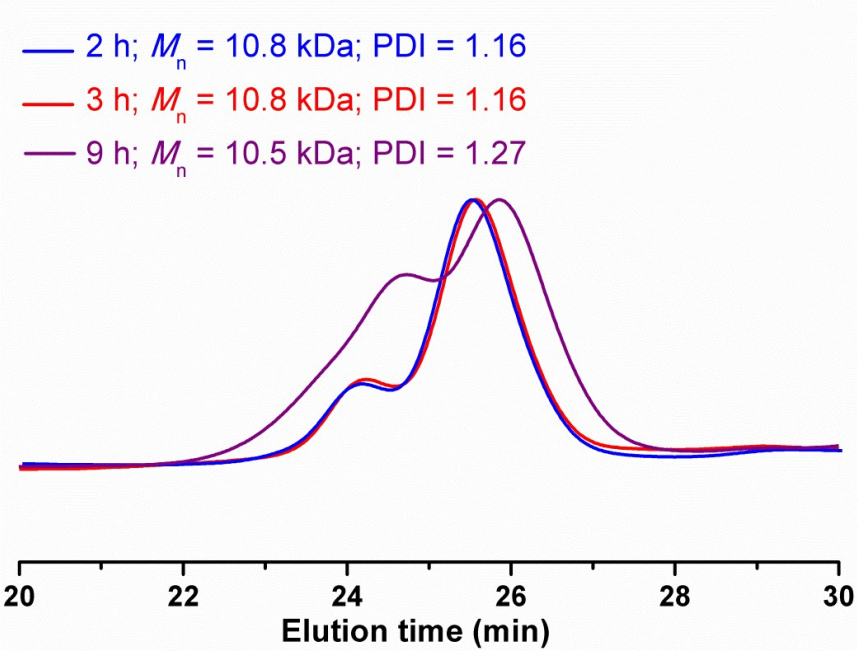

Figure S17. The GPC evolution plots of the resultant poly(PA-*alt*-CHO) obtained from a single polymerization reaction. With time prolonging, a bimodal GPC trace and wider distribution were observed.

The observation attributed to chain transfer and transesterification.

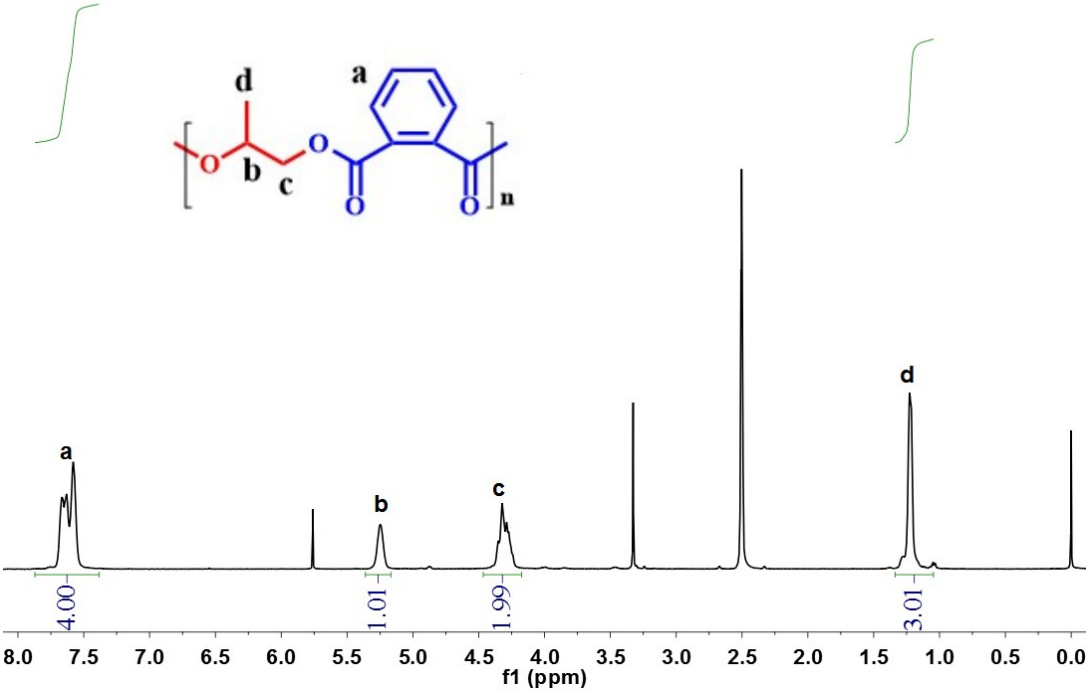

Figure S18. ^{1}H NMR spectrum of the resultant poly(PA-*alt*-PO) in DMSO-*d*6.

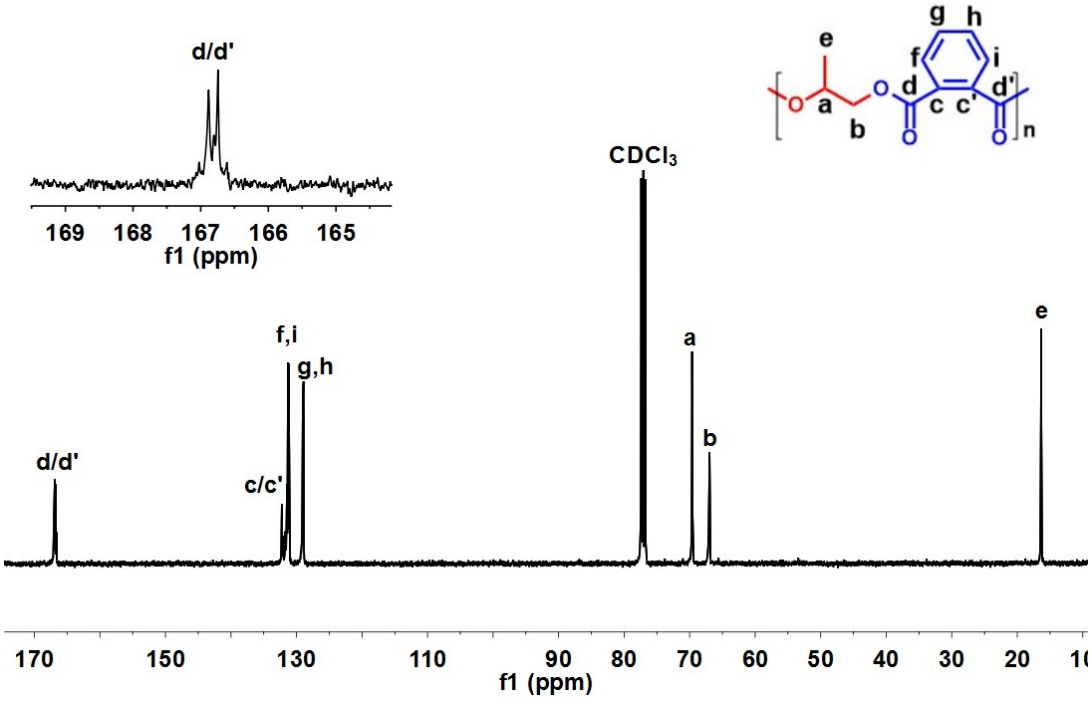

Figure S19. ^{13}C NMR spectrum of the resultant poly(PA-*alt*-s-PO) in $CDCl_3$.

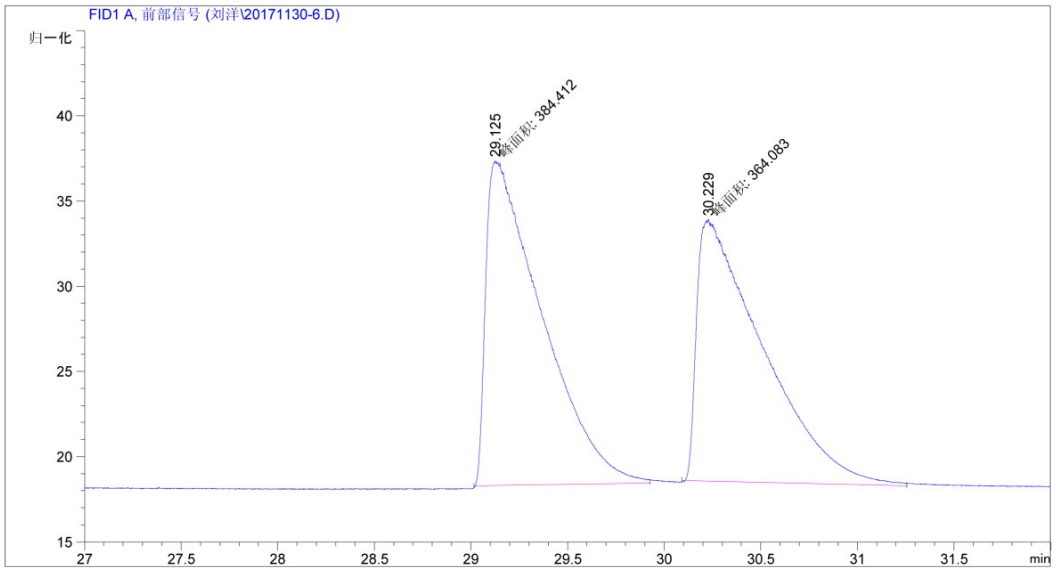

==========

面积百分比报告

==========

排序 : 信号
乘积因子: : 1.0000
稀释因子: : 1.0000
内标使用乘积因子和稀释因子

信号 1: FID1 A, 前部信号

峰 #	保留时间 [min]	类型	峰宽 [min]	峰面积 [pA*s]	峰高 [pA]	峰面积 %
1	29.125	MM	0.3362	384.41193	19.05661	51.35795
2	30.229	MM	0.3961	364.08347	15.32120	48.64205
总量 :				748.49539	34.37781	

Figure S20. GC analysis of the *racemic* 1,2-propanediol resulting from the hydrolysis of poly(PA-*alt*-*rac*PO).

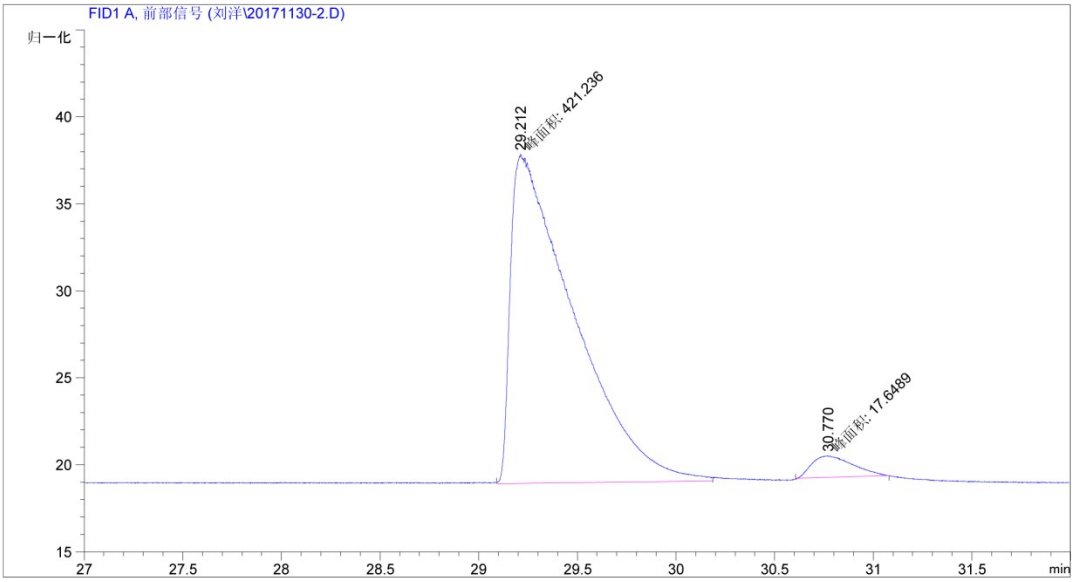

==========

面积百分比报告

==========

排序 : 信号
乘积因子: : 1.0000
稀释因子: : 1.0000
内标使用乘积因子和稀释因子

信号 1: FID1 A, 前部信号

峰 #	保留时间 [min]	类型	峰宽 [min]	峰面积 [pA*s]	峰高 [pA]	峰面积 %
1	29.212	MM	0.3714	421.23593	18.90334	95.97869
2	30.770	MM	0.2386	17.64892	1.23271	4.02131

总量 : 438.88485 20.13605

Figure S21. GC analysis of the *S*-enriched 1,2-propanediol (*ee* = 91.96%) resulting from the hydrolysis of poly(PA-*alt*-*S*PO).

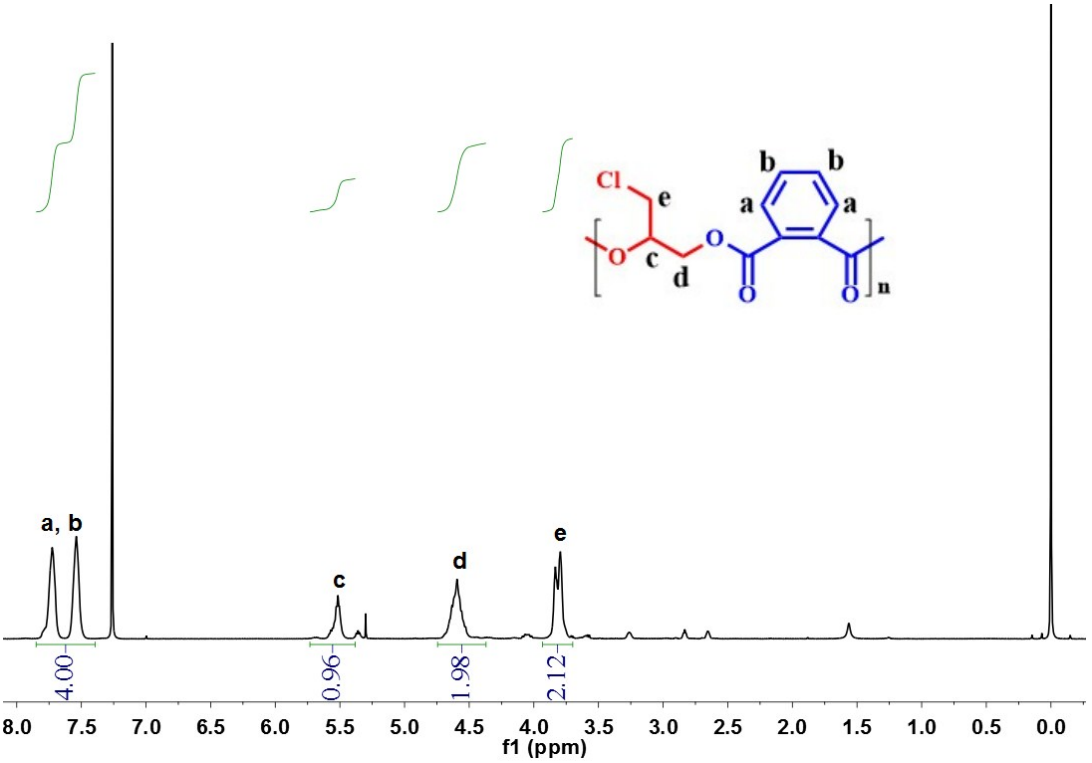

Figure S22. ^{1}H NMR spectrum of the resultant poly(PA-*alt*-ECH) in $CDCl_3$.

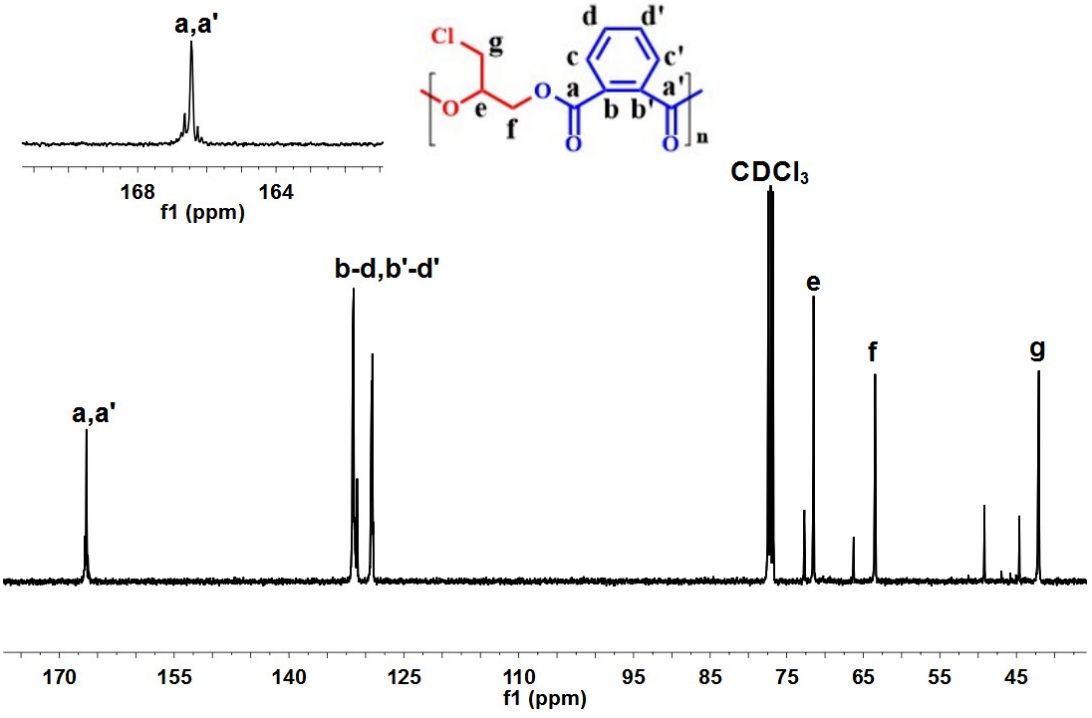

Figure S23. ^{13}C NMR spectrum of the resultant poly(PA-*alt*-ECH) in $CDCl_3$.

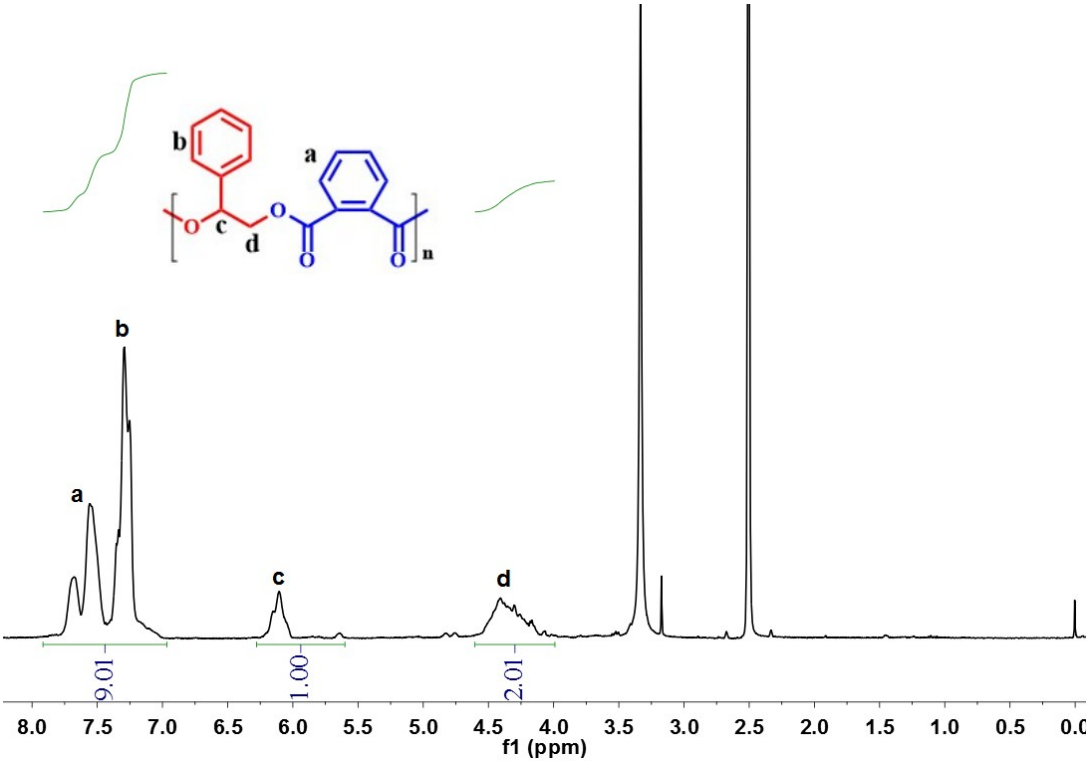

Figure S24. [1]H NMR spectrum of the resultant poly(PA-*alt*-SO) in DMSO-*d*6.

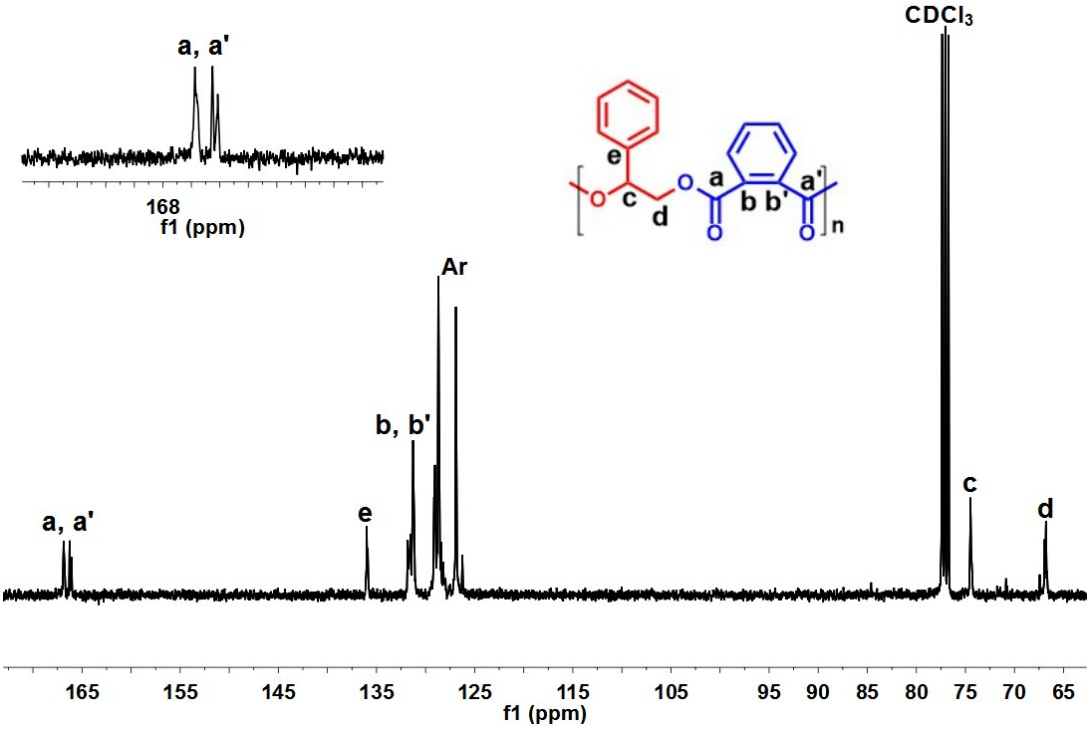

Figure S25. [13]C NMR spectrum of the resultant poly(PA-*alt*-SO) in $CDCl_3$.

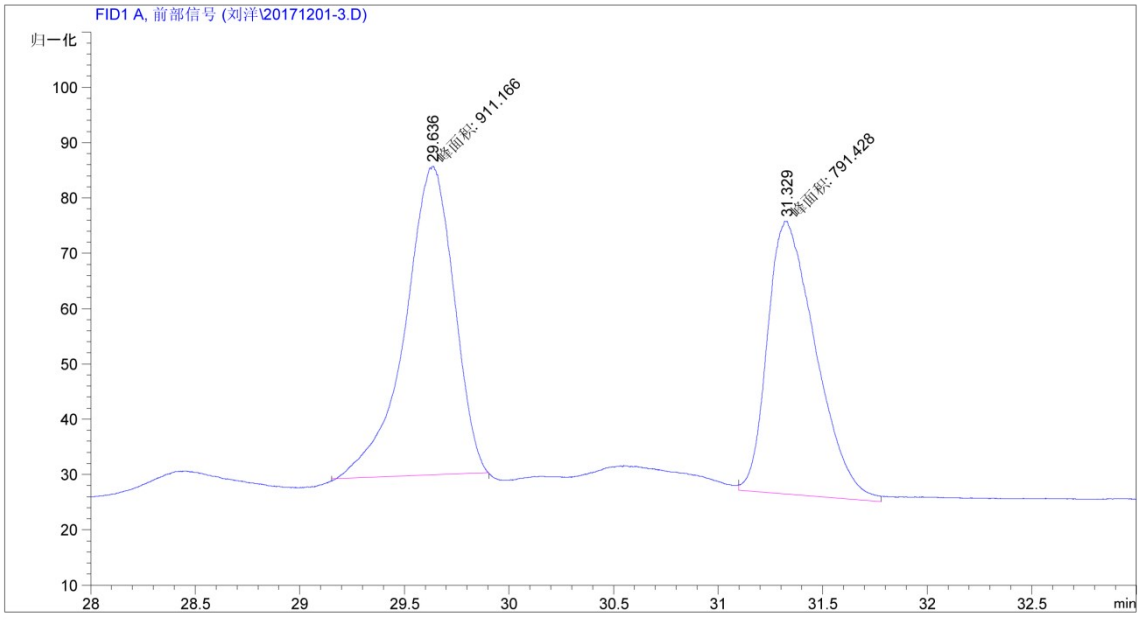

==========

面积百分比报告

==========

排序 : 信号
乘积因子: : 1.0000
稀释因子: : 1.0000
内标使用乘积因子和稀释因子

信号 1: FID1 A, 前部信号

峰 #	保留时间 [min]	类型	峰宽 [min]	峰面积 [pA*s]	峰高 [pA]	峰面积 %
1	29.636	MM	0.2722	911.16626	55.78238	53.51634
2	31.329	MM	0.2674	791.42816	49.33087	46.48366

总量 : 1702.59442 105.11325

Figure S26. GC analysis of the *racemic* styrene glycol resulting from the hydrolysis of poly(PA-*alt*-*rac*SO).

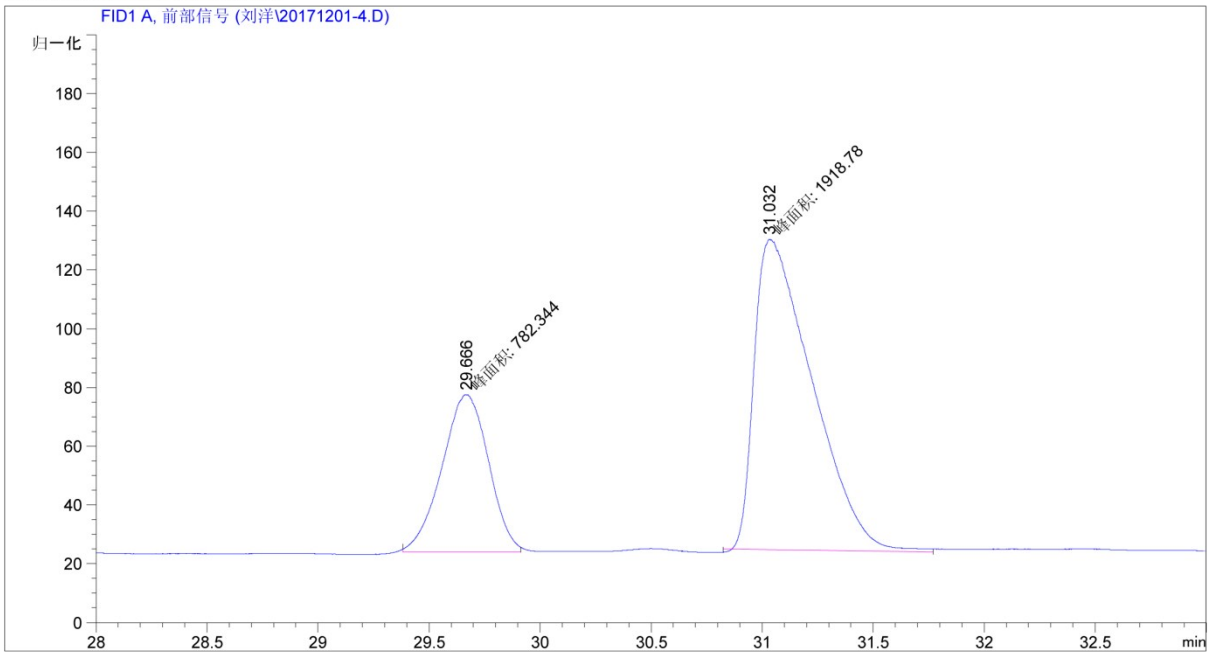

==========

面积百分比报告

==========

排序 : 信号
乘积因子: : 1.0000
稀释因子: : 1.0000
内标使用乘积因子和稀释因子

信号 1: FID1 A, 前部信号

峰 #	保留时间 [min]	类型	峰宽 [min]	峰面积 [pA*s]	峰高 [pA]	峰面积 %
1	29.666	MM	0.2431	782.34363	53.64128	28.96365
2	31.032	MM	0.3028	1918.77917	105.60246	71.03635
总量 :				2701.12280	159.24374	

Figure S27. GC analysis of the *S*-enriched styrene glycol (*ee* = 42.08%) resulting from the hydrolysis of poly(PA-*alt*-*S*SO). The lower *ee* value than PO attributed to the electron-withdrawing phenyl group, in which methine of SO had a higher probability to ring-open by nucleophilic attack of Lewis bases or chain growing species.

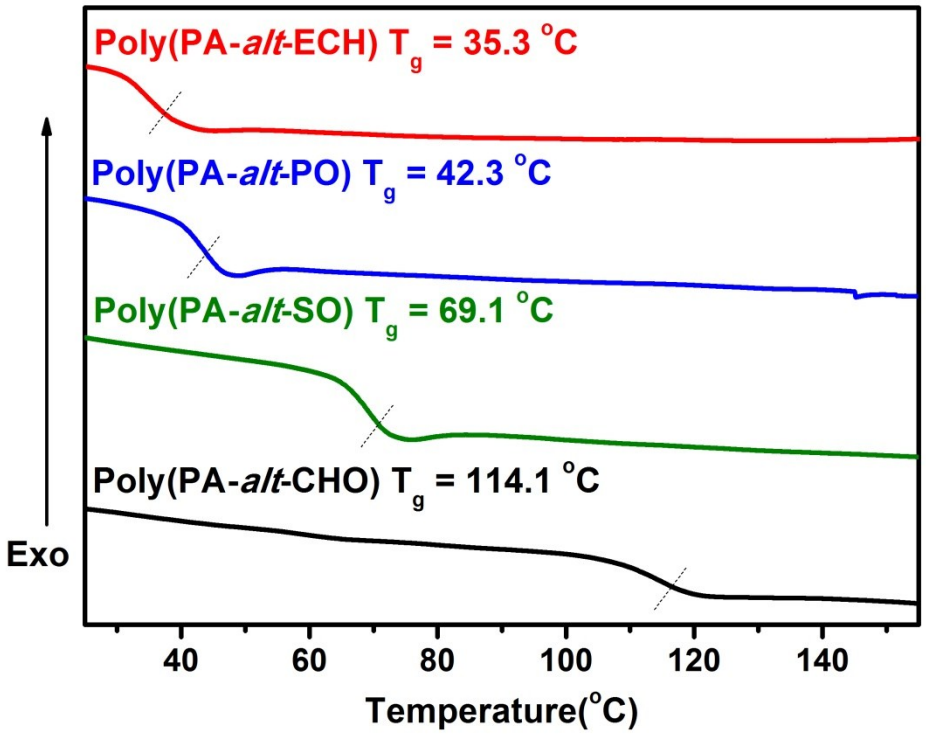

Figure S28. DSC plots of PA-based semiaromatic polyesters. A wide range of glass transition temperature (T_g) could be achieved by simply tuning comonomers.

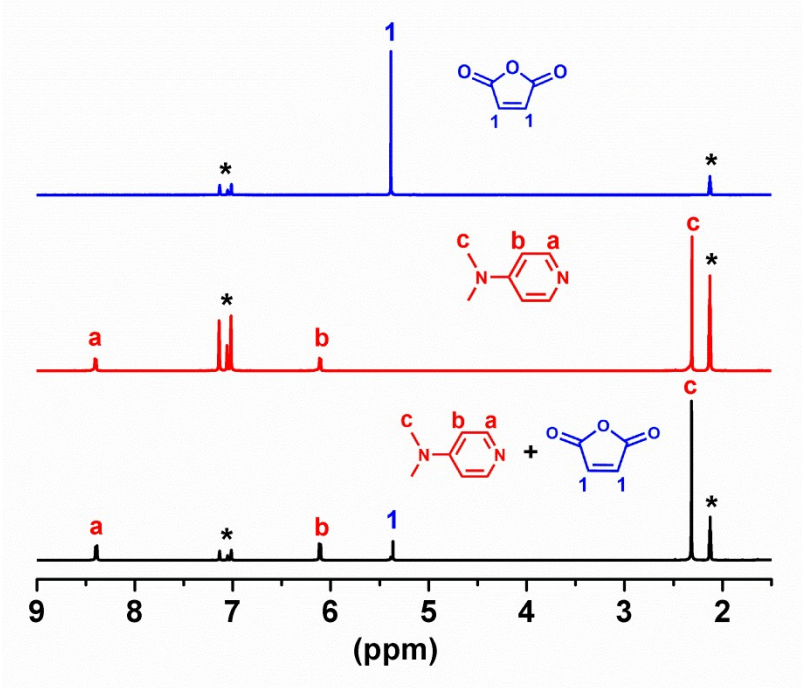

Figure S29. ^{1}H NMR spectra of MA and equivalent DMAP in toluene-d_8. Obviously, α-H signals of MA at 5.39 ppm did not disappear; suggesting that deprotonation between MA and DMAP was suppressed.

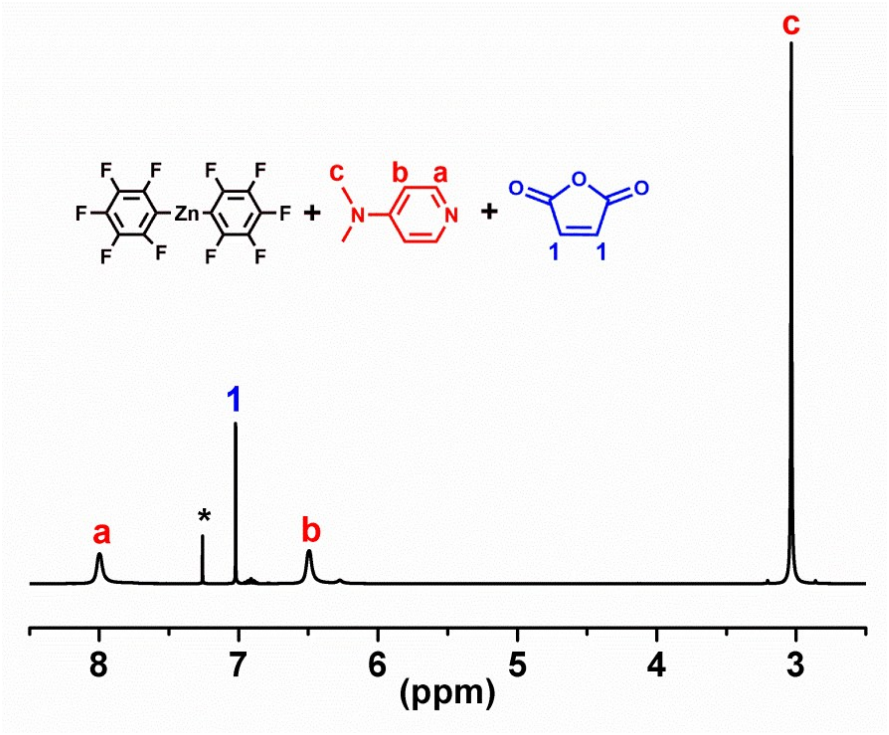

Figure S30. ^{1}H NMR spectrum of $Zn(C_6F_5)_2$/DMAP/MA with 1:2:1 molar ratio in $CDCl_3$. The signal at 7.05 ppm attributed to the α-H of MA remained as it was, suggesting the presence of $Zn(C_6F_5)_2$ also inhibited deprotonation.

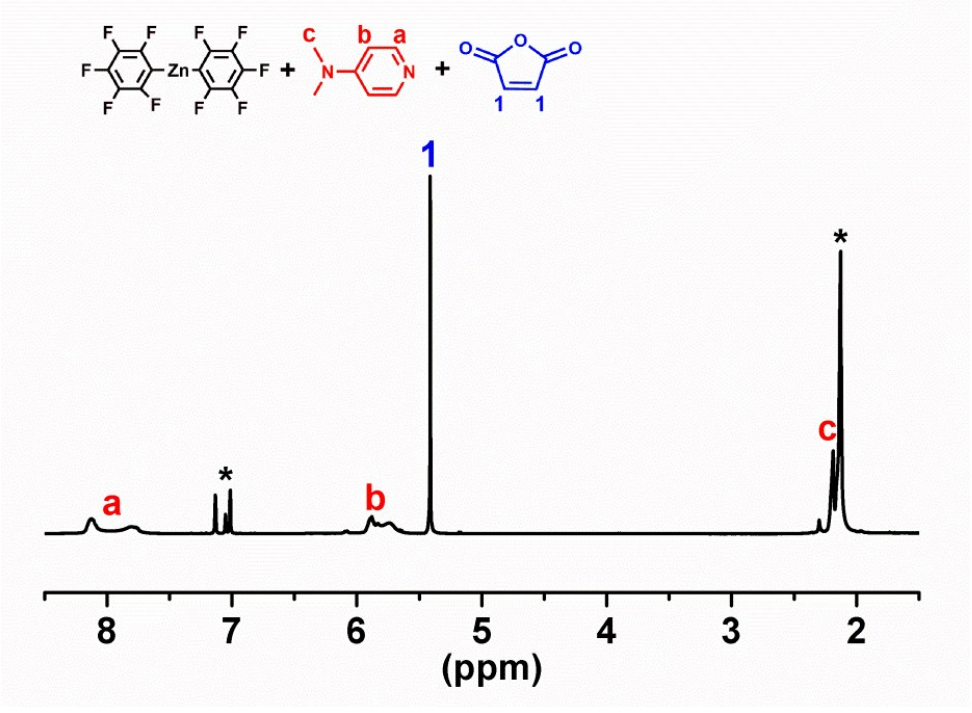

Figure S31. ^{1}H NMR spectrum of $Zn(C_6F_5)_2$/DMAP/MA with 1:2:1 molar ratio in toluene-d_8.

Table S2. Ring-opening alternating copolymerization of anhydrides and CHO catalyzed by $Zn(C_6F_5)_2$/DMAP Lewis pair.[a]

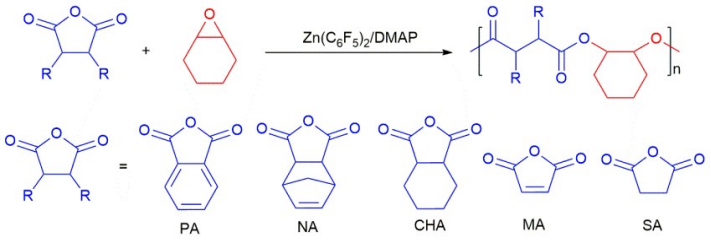

entry	Anhydride	Solvent	LA/LB/Anhydride/CHO	t (h)	Conv. (%)[b]	Alternating degree (%)[c]	M_n (kDa)[d]	PDI[d]
1	NA	bulk	1:2:100:500	4	83	96	7.2	1.26
2	NA	xylene	1:2:100:100	6	41	>99	3.9	1.16
3	NA	oDCB	1:2:100:100	6	24	94	2.1	1.14
4	CHA	oDCB	1:2:100:100	4	33	88	-[e]	-[e]
5	MA	bulk	1:2:100:500	1	gel	-[e]	-[e]	-[e]
6	PA	DHN	1:2:100:100	2	96	>99	7.3	1.19
7	NA	DHN	1:2:100:100	6	53	>99	4.2	1.13
8	CHA	DHN	1:2:100:100	4	94	93	9.1	1.19
9	SA	DHN	1:2:100:100	2	97	96	10.1	1.20

[a]Unless otherwise mentioned, the copolymerization reactions were carried out at 110 °C. [b]The conversion of anhydride was determined by ^{1}H NMR spectrum. [c]Alternating degree was determined by ^{1}H NMR spectroscopy by integrating ester signals and ether signals. [d]M_n and PDI were determined by GPC analysis in THF calibrated by PS standards. [e]Not defined.

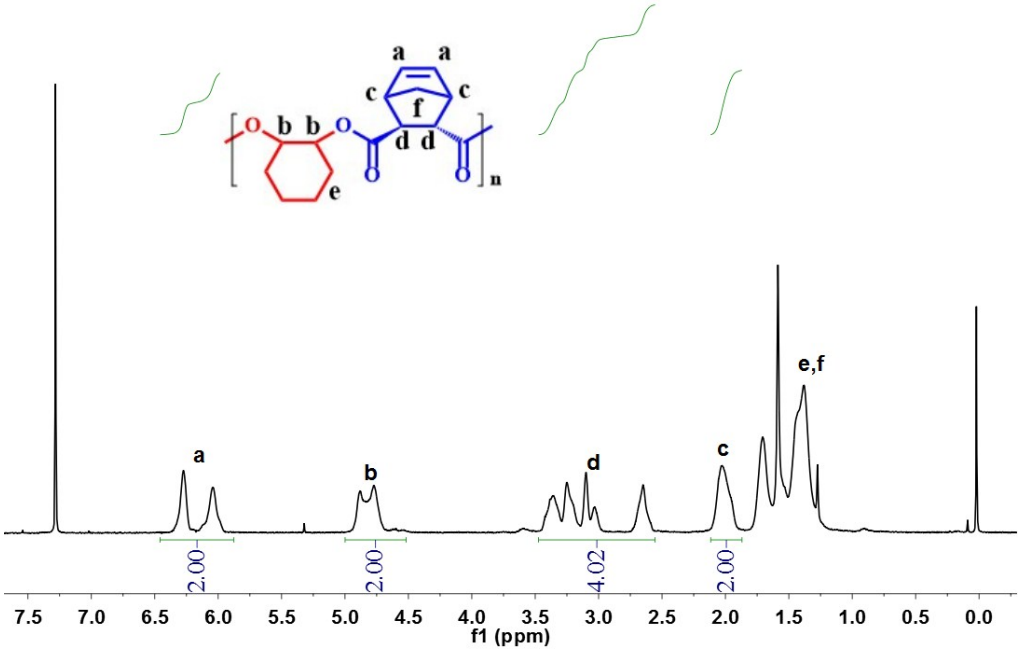

Figure S32. ^{1}H NMR spectrum of the resultant poly(NA-*alt*-CHO) in $CDCl_3$. A *trans*-polyester was

obtained from this system because of epimerization.

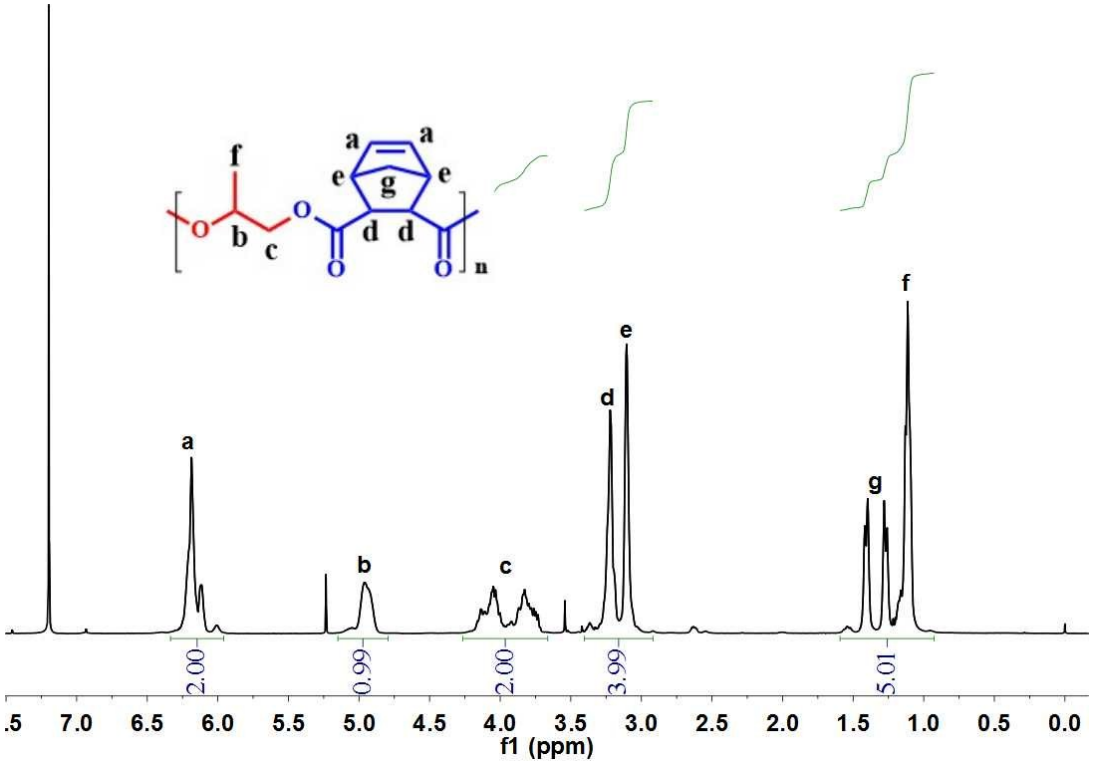

Figure S33. ^{1}H NMR spectrum of the resultant poly(NA-*alt*-PO) in $CDCl_3$.

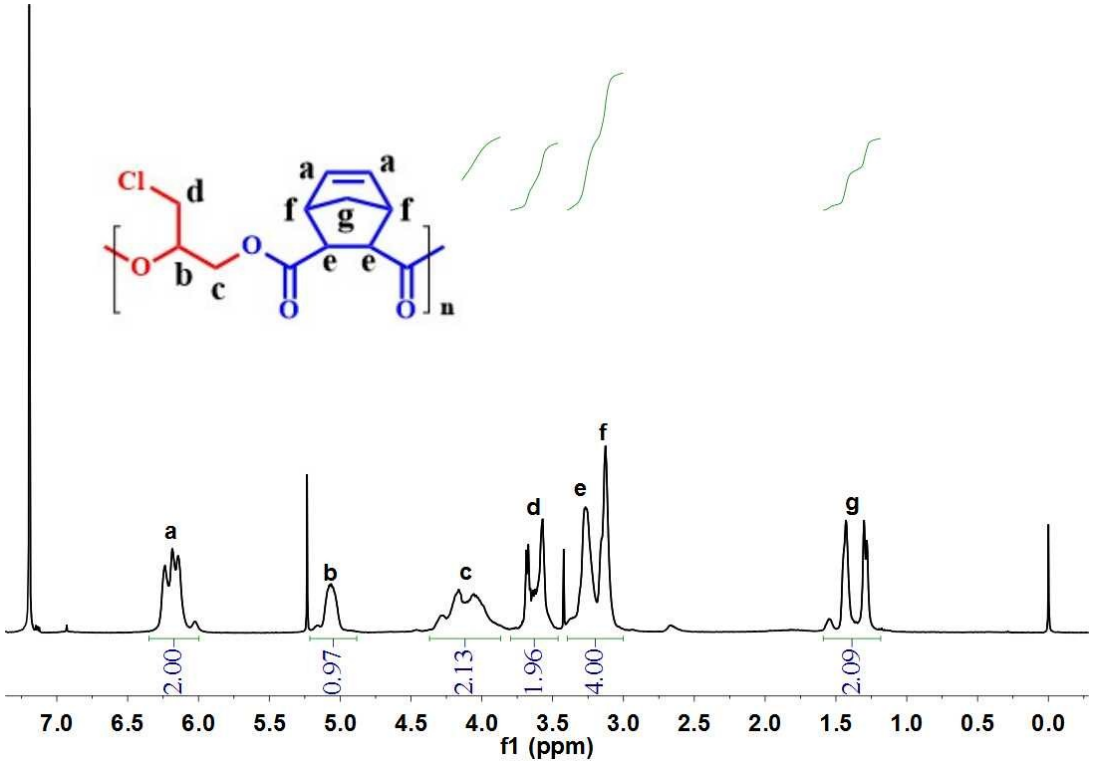

Figure S34. ^{1}H NMR spectrum of the resultant poly(NA-*alt*-ECH) in $CDCl_3$.

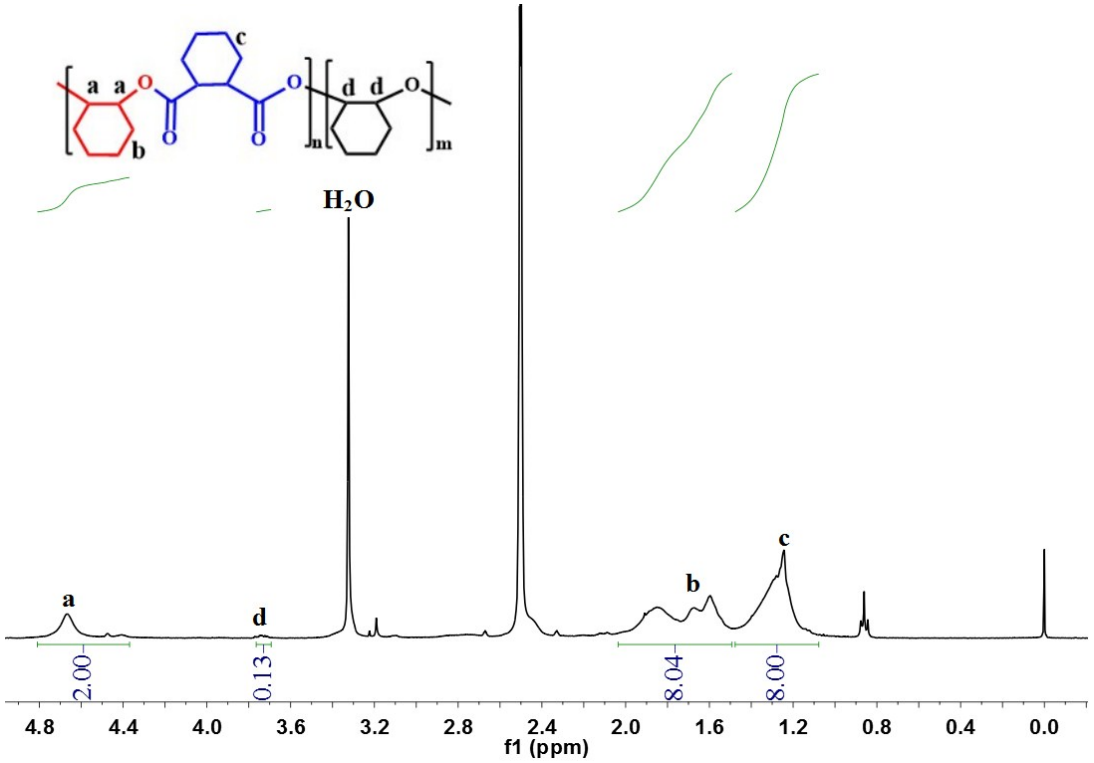

Figure S35. ^{1}H NMR spectrum of the resultant poly(CHA-*alt*-CHO) in DMSO-*d*6.

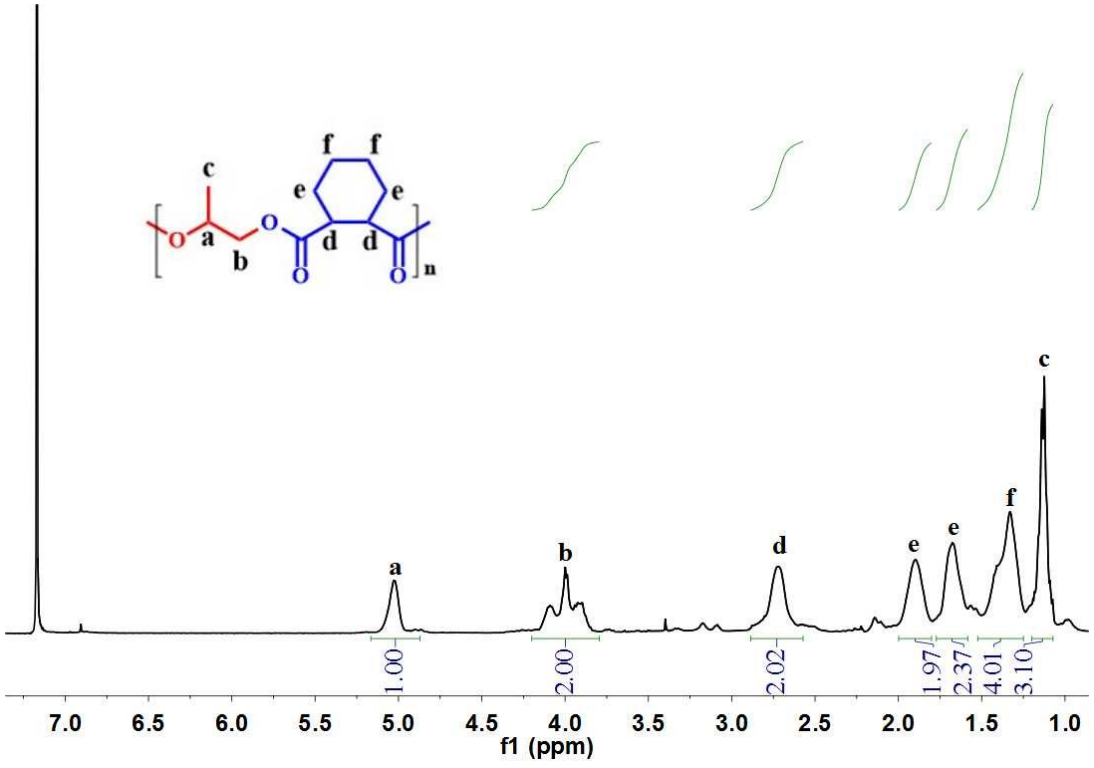

Figure S36. ^{1}H NMR spectrum of the resultant poly(CHA-*alt*-PO) in $CDCl_3$.

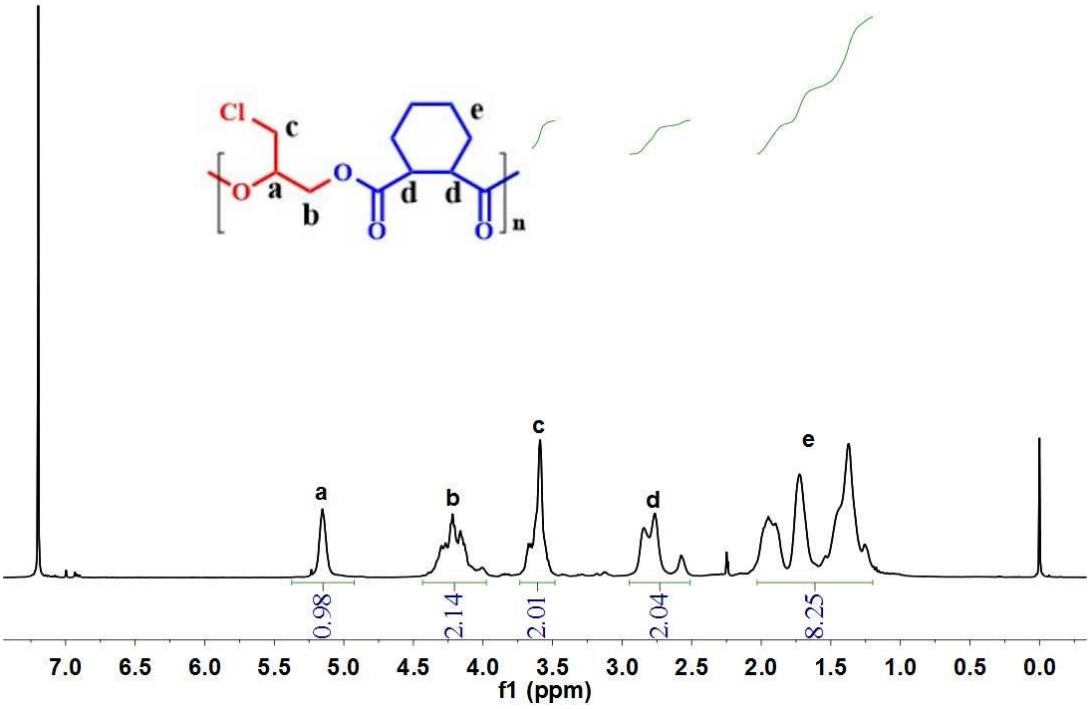

Figure S37. ^{1}H NMR spectrum of the resultant poly(CHA-*alt*-ECH) in $CDCl_3$.

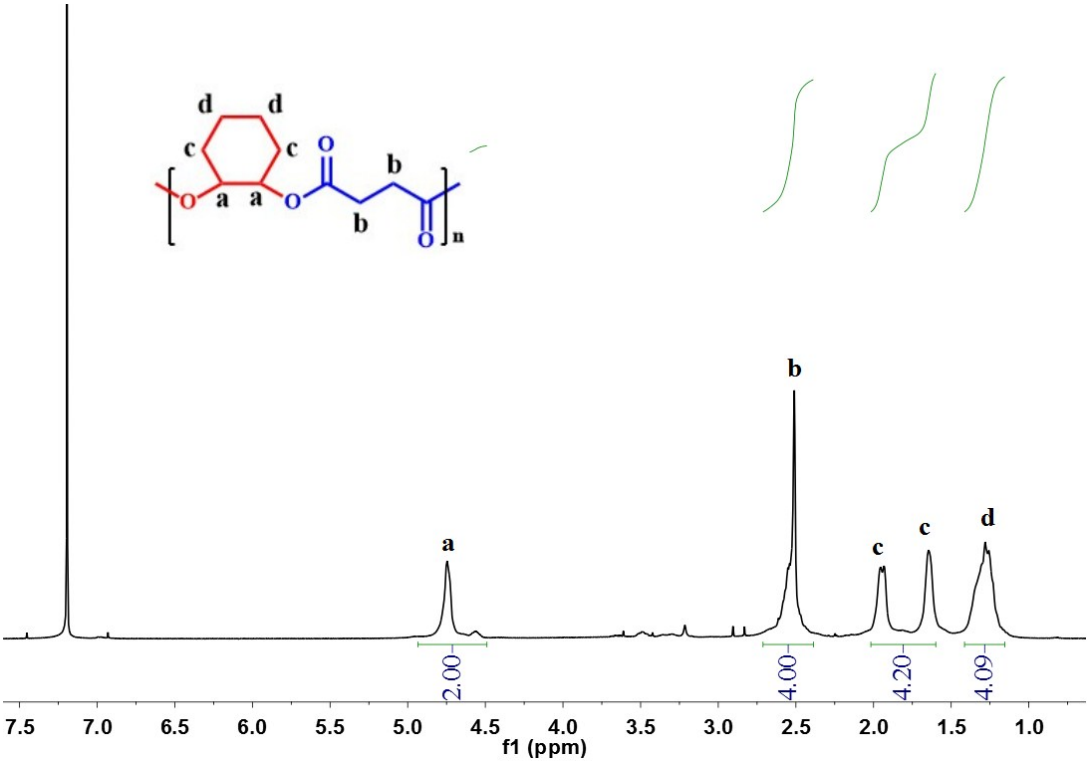

Figure S38. ^{1}H NMR spectrum of the resultant poly(SA-*alt*-CHO) in $CDCl_3$.

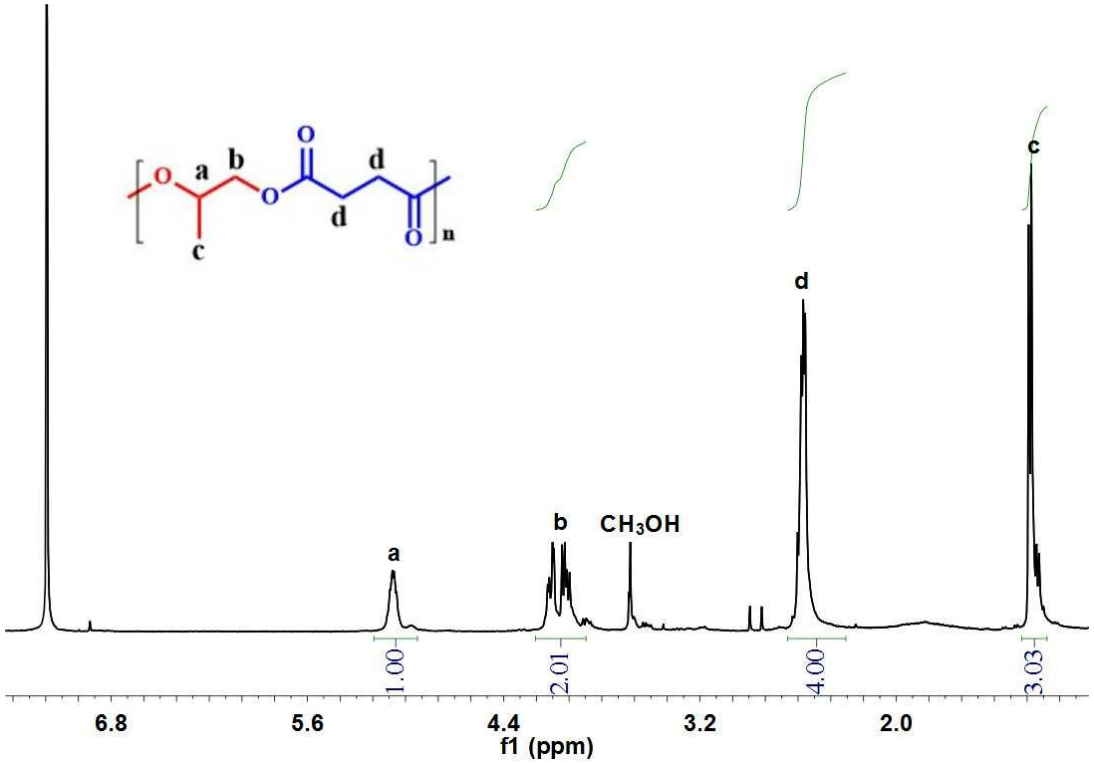

Figure S39. ^{1}H NMR spectrum of the resultant poly(SA-*alt*-PO) in $CDCl_3$.

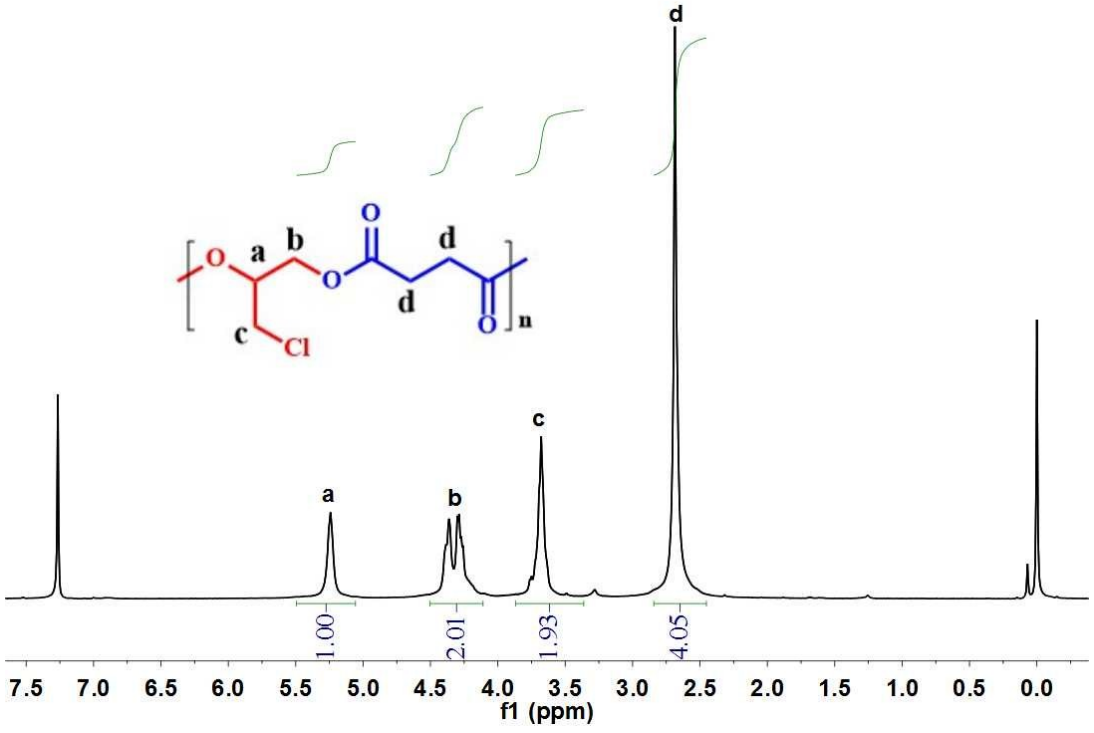

Figure S40. ^{1}H NMR spectrum of the resultant poly(SA-*alt*-ECH) in $CDCl_3$.

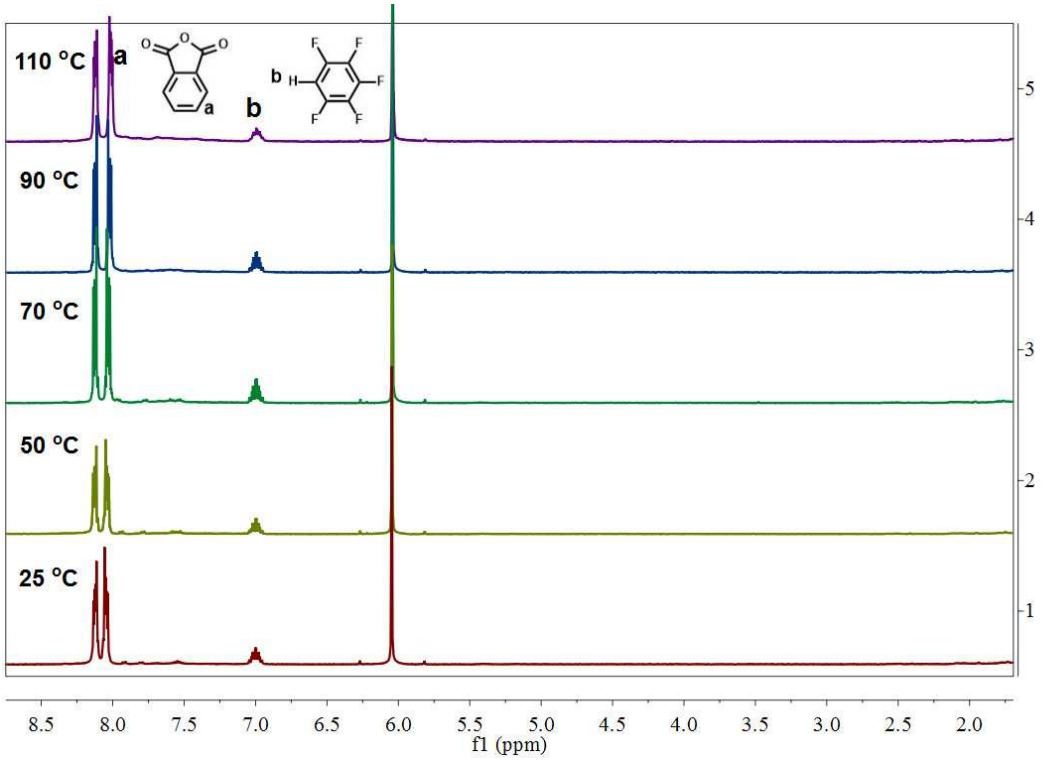

Figure S41. VT ^{1}H NMR spectra of $Zn(C_6F_5)_2$/PA with the molar ratio of 1:1 in $C_2D_2Cl_4$. The result didn't give extra information spread the range of all chemical shifts.

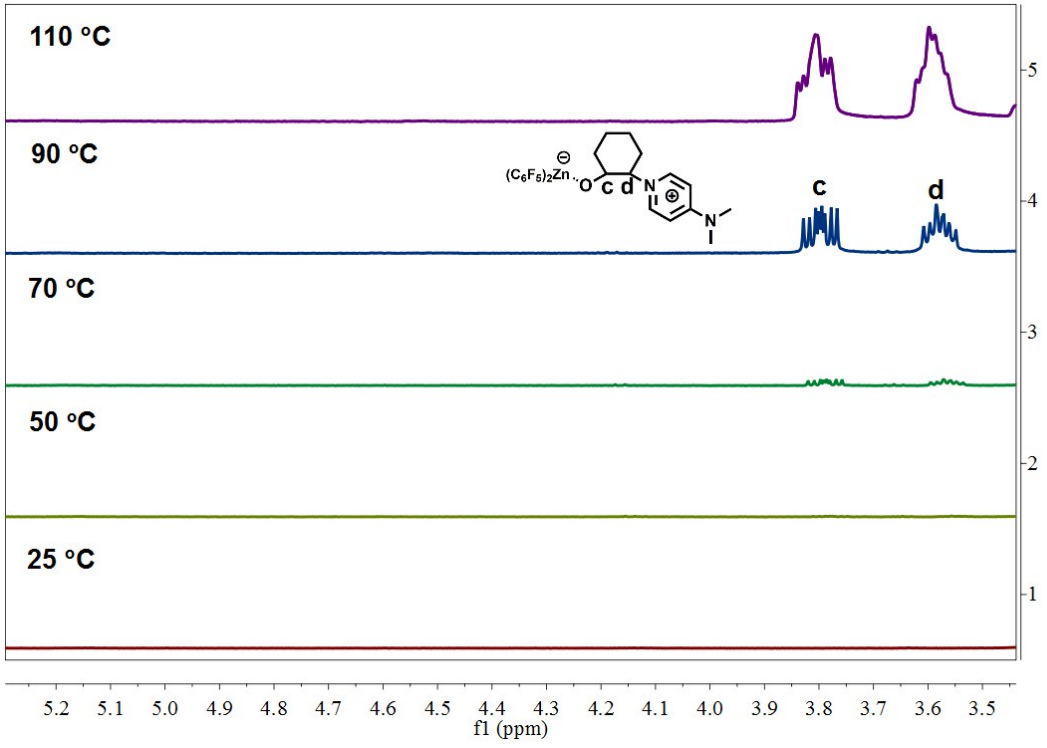

Figure S42. VT ^{1}H NMR spectra of $Zn(C_6F_5)_2$/DMAP/CHO with the molar ratio of 1:1:1 in $C_2D_2Cl_4$.

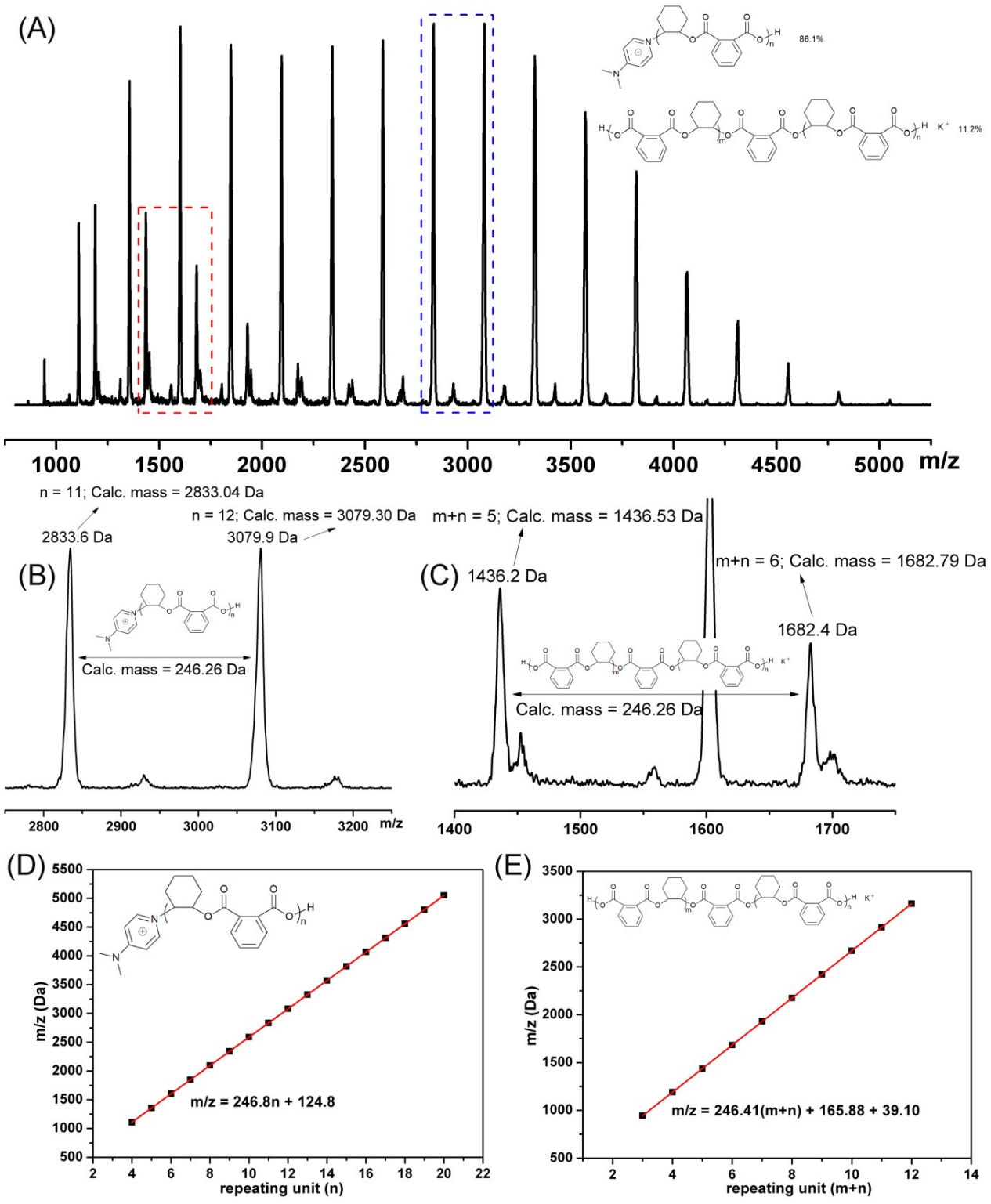

Figure S43. (a) Positive ion MALDI-TOF MS of poly(PA-*alt*-CHO) in a low PA conversion (44%, PA was sublimed one time) precipitated in *n*-hexane without quenching. (b) A detail of blue grid in (a) with calculated and exact masses. (c) A detail of red grid in (a) with calculated and exact masses. (d) The fitting relationship of M_n of DMAP-terminated species *vs* repeating unit. (e) The fitting relationship of M_n of PA-centered species *vs* repeating unit.

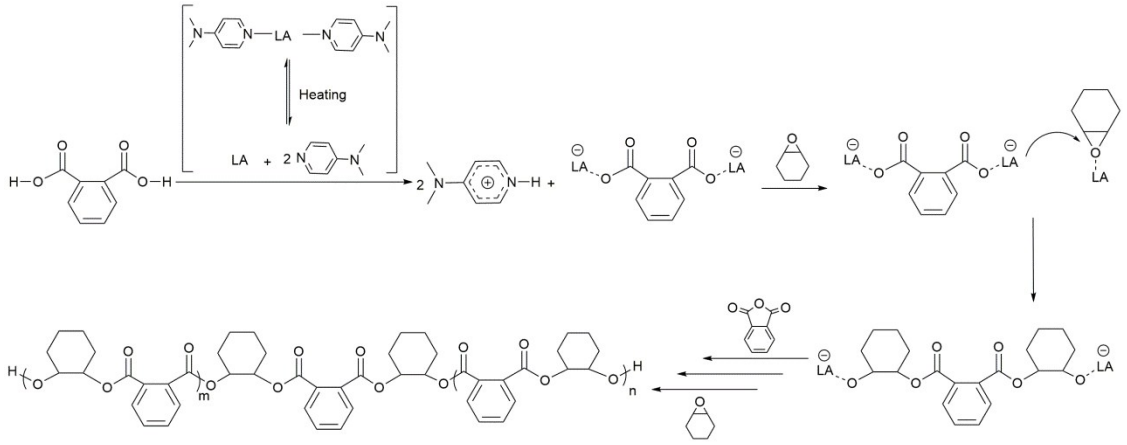

Scheme S1. Proposed mechanism schematic illustration of chain initiation and propagation catalyzed by slight phthalic acid[6] and additional Lewis pair. In the presence of dissociated Lewis pair, organic base has a trend to capture the active proton in phthalic acid to form carboxylate nucleophile species. And then, epoxide activated by LA would ring-open with carboxylate attacking. Finally, anhydride and epoxide alternatively inserted into propagating chain.

References

1 X. Q. Li, B. Wang, H. Y. Ji and Y. S. Li, *Catal. Sci. Technol.*, 2016, **6**, 7763-7772.

2 J. Li, Y. Liu, W. M. Ren and X. B. Lu, *J. Am. Chem. Soc.*, **2016**, *138*, 11493−11496.

3 R. M. Hanson, *Chem. Rev.*, 1991, 91, 437−475.

4 S. Huijser, E. Hosseini Nejad, R. Sablong, C. de Jong, C. E. Koning and R. Duchateau, *Macromolecules*, 2011, **44**, 1132-1139.

5 P. K. Saini, C. Romain, Y. Zhu and C. K. Williams, *Polym. Chem.*, 2014, **5**, 6068-6075.

6 Z. Hošťálek, O. Trhlíková, Z. Walterová, T. Martinez, F. Peruch, H. Cramail and J. Merna, *Eur. Polym. J.*, 2017, **88**, 433-447.